Cloud water composition during HCCT-2010: Scavenging efficiencies, solute concentrations, and droplet size dependence of inorganic ions and dissolved organic carbon

D. van Pinxteren[1], K.W. Fomba[1], S. Mertes[1], K. Müller[1], G. Spindler[1], J. Schneider[2], T. Lee[3*], J. Collett[3], and H. Herrmann[1]

[1] Leibniz-Institut für Troposphärenforschung (TROPOS), Permoserstr. 15, 04318 Leipzig, Germany

[2] Max Planck Institute for Chemistry, Hahn-Meitner-Weg 1, 55128 Mainz, Germany

[3] Colorado State University, Department of Atmospheric Science, Fort Collins, CO 80523, USA

*now at: Hankuk University of Foreign Studies, Department of Environmental Sciences, Yongin, South Korea

Correspondence to: H. Herrmann (herrmann@tropos.de)

Revised version, submitted January 2016

Abstract

Cloud water samples were taken in September/October 2010 at Mt. Schmücke in a rural, forested area in Germany during the Lagrange-type Hill Cap Cloud Thuringia 2010 (HCCT-2010) cloud experiment. Besides bulk collectors, a 3-stage and a 5-stage collector were applied and samples were analysed for inorganic ions (SO_4^{2-},NO_3^-, NH_4^+, Cl^-, Na^+, Mg^{2+}, Ca^{2+}, K^+), H_2O_2 (aq), S(IV), and dissolved organic carbon (DOC). Campaign volume-weighted mean concentrations were 191, 142, and 39 µmol L^{-1} for ammonium, nitrate, and sulfate, respectively, between 4 and 27 µmol L^{-1} for minor ions, 5.4 µmol L^{-1} for H_2O_2 (aq),

1.9 µmol L^{-1} for S(IV), and 3.9 mgC L^{-1} for DOC. The concentrations compare well to more recent European cloud water data from similar sites. On a mass basis, organic material (as DOC * 1.8) contributed 20-40% (event means) to total solute concentrations and was found to have non-negligible impact on cloud water acidity. Relative standard deviations of major ions were 60-66% for solute concentrations and 52-80% for cloud water loadings (CWLs). The similar variability of solute concentrations and CWLs together with the results of back trajectory analysis and principal component analysis, suggests that concentrations in incoming air masses (i.e. air mass history), rather than cloud liquid water content (LWC) was the main factor controlling bulk solute concentrations for the cloud studied. Droplet effective radius was found to be a somewhat better predictor for cloud water total ionic content (TIC) than LWC, even though no single explanatory variable can fully describe TIC (or solute concentration) variations in a simple functional relation due to the complex processes involved. Bulk concentrations typically agreed within a factor of 2 with co-located measurements of residual particle concentrations sampled by a counterflow virtual impactor (CV) and analysed by an aerosol mass spectrometer (AMS), with the deviations being mainly caused by systematic differences and limitations of the approaches (such as outgassing of dissolved gases during residual particle sampling). Scavenging efficiencies (SEs) of aerosol constituents were 0.56-0.94, 0.79-0.99, 0.71-98, and 0.67-0.92 for SO_4^{2-}, NO_3^-, NH_4^+, and DOC, respectively, when calculated as event means with in-cloud data only. SEs estimated using data from an upwind site were substantially different in many cases, revealing the impact of gas-phase uptake (for volatile constituents) and mass losses across Mt. Schmücke likely due to physical processes such as droplet scavenging by trees and/or entrainment. Drop size-resolved cloud water concentrations of major ions SO_4^{2-}, NO_3^-, and NH_4^+ revealed two main profiles: decreasing concentrations with increasing droplet size and "U"-shapes. In contrast, profiles of typical coarse particle mode minor ions were often increasing with increasing drop size, highlighting the importance of a species' particle concentration size distribution for the development of size-resolved solute concentration patterns. Concentration differences between droplet size classes were typically <2 for major ions from the 3-stage collector and somewhat more pronounced from the 5-stage collector, while they were much larger for minor ions. Due to a better separation of droplet populations, the 5-stage collector was capable of resolving some features of solute size dependencies not seen in the 3-stage data, especially sharp concentration increases (up to a factor of 5-10) in the smallest droplets for many solutes.

1 Introduction

Clouds represent an important part of the atmospheric multiphase system. Uptake of gases, dissolution of cloud condensation nuclei (CCN) constituents, and chemical reactions lead to complex compositions of their aqueous phase, which are highly variable in time and space and droplet size. Knowledge of these compositions and their variability is crucial for understanding a number of important processes in the atmosphere, including droplet activation and growth (e.g. Taraniuk et al., 2008; Facchini et al., 1999), formation and transformation of compounds (e.g. Herrmann et al., 2015; Fahey et al., 2005), production and consumption of important oxidants (e.g. Whalley et al., 2015; Marinoni et al., 2011), or transport and deposition of pollutants (e.g. Vet et al., 2014; Fowler et al., 2009). The present contribution presents results of cloud water chemical composition and related measurements during the Hill Cap Cloud Thuringia 2010 (HCCT-2010) experiment, performed in autumn 2010 at Mt. Schmücke, Germany. It focuses on the aspects of i) main drivers of bulk cloud water solute concentrations, ii) scavenging efficiencies of aerosol constituents, and iii) size-resolved droplet composition, which will be introduced here.

Whether and to what extent *solute concentrations are controlled by LWC* has been debated in the literature. Both Möller et al. (1996) and Elbert et al. (2000) concluded from their studies that LWC was the main parameter in controlling cloud water total ionic content (TIC) and that this relationship could be described by a power law function. From a comprehensive literature survey, Elbert et al. (2000) concluded that at any given site the cloud water loading (CWL, the product of solute concentrations and LWC) would be a fairly constant value (with "fairly constant" being interpreted as max / mean ratio < 5). In a discussion of this proposition (Kasper-Giebl, 2002; Elbert et al., 2002), Kasper-Giebl (2002) demonstrated that a constant CWL would imply either constant scavenging efficiencies and substance concentrations in air, or opposite trends of these two parameters, neither of which can be generally regarded as true. More recently, Aleksic and Dukett (2010) showed for a very large dataset, that the relationship of TIC ~ LWC cannot be described by a simple function, but rather by a series of exponential distributions of TIC whose means values decrease with increasing LWC. These authors as well conclude that CWL is a stochastic quantity and thus cannot be a constant. In section 3.3.2 of this work the parameters controlling bulk cloud water solute concentrations

are studied for the comparatively uniform conditions during HCCT-2010 (with its identical site, season and wind sector during sampling).

Scavenging efficiencies (SEs) indicate how much of a compounds' total concentration is recovered in the cloud liquid phase after cloud formation. Different approaches for its calculation exist. Cloud water concentrations and interstitial particulate and/or gaseous concentrations have been used to derive in-cloud scavenging efficiencies of non-volatile or (semi)-volatile compounds (Sellegri et al., 2003; Acker et al., 2002; Hitzenberger et al., 2000; Kasper-Giebl et al., 2000; Daum et al., 1984). Alternatively, cloud concentrations can be related to total particulate (and/or gaseous) concentrations upwind of a cloud (van Pinxteren et al., 2005; Svenningsson et al., 1997; Leaitch et al., 1986; Hegg et al., 1984) or before cloud/fog onset (Gilardoni et al., 2014; Collett et al., 2008; Noone et al., 1992). In the ideal case of a "closed system" with conserved masses, all approaches would lead to the same scavenging efficiencies. However, as real clouds and fogs are open and dynamic systems, heavily interacting with their physical and chemical environment, the different approaches might lead to different results and comparing these might allow for insights into important processes taking place in the cloud/fog system. In the present study, many (though not all) of the phases relevant for the concentrations of major cloud constituents (sulfate, nitrate, ammonium, DOC) have been measured both upwind and inside of clouds at the Schmücke and are used to calculate and compare scavenging efficiencies derived from different approaches (section 3.3.4).

In clouds, *solute concentrations typically vary across droplet size* (Bator and Collett, 1997; Rao and Collett, 1995), which has significant implications for chemical reactions in droplets (Fahey et al., 2005; Reilly et al., 2001; Hoag et al., 1999; Gurciullo and Pandis, 1997) and deposition behaviour of solutes (Moore et al., 2004b; Collett et al., 2001; Bator and Collett, 1997). A conceptual model developed by Ogren et al. (1992) qualitatively describes the variation of non-volatile solute concentrations with cloud drop size in 3 different drop size regions: Region I ranges from < 1µm to approx. 5 µm drop diameter (exact size range strongly depends on cloud properties) and contains freshly activated (or non-activated) droplets close to their equilibrium size at the prevailing supersaturation. In this so-called "equilibrium growth" region, solute concentrations sharply decrease with increasing drop size, because at their critical diameter, larger droplets are more dilute than smaller ones as a result of the interactions between the Kelvin and the Raoult effect (Pruppacher and Klett,

2010; Ogren and Charlson, 1992). Region II, ranging from approx. 5 – 50 µm, represents droplets which have freely grown by water condensation beyond their critical size. In this "condensation growth" region, solute concentrations increase with increasing drop size, because small drops grow faster than large drops (r^{-1} growth law), i.e. large drops experience less dilution as compared to smaller ones. In region III, above approx. 50 µm in diameter, coalescence of drops becomes important. As larger drops collide more efficiently with smaller (i.e. more diluted) ones, solute concentrations decrease with increasing drop size in this "coalescence growth" region.

In more detailed numerical simulations, Schell et al. (1997) studied parameters determining non-volatile solute concentrations in different droplet sizes. Their results show size dependencies which are in principle consistent with the three regions in the conceptual model of Ogren et al. (1992). However, the exact shape of the curve strongly depends on several parameters like the droplet growth time (cloud age), the width of the CCN number distribution (e.g. presence of coarse particles), and the soluble fraction of input aerosol particles. In some cases, the concentration increase in the Ogren et al. region II can diminish to the point of constantly decreasing solute concentrations with increasing droplet sizes nearly over the full droplet size range.

These model results illustrate the complexity of solute concentration drop size dependencies, which is even increased in reality by many factors such as gas-phase uptake of soluble material, chemical reactions in droplets, size-dependent composition and variable mixing state of input aerosol, entrainment processes, and inhomogeneous fields of supersaturation, i.e. different histories of individual droplets (Flossmann and Wobrock, 2010; Ogren and Charlson, 1992). In addition, available instrumentation for size-resolved droplet sampling usually integrates both over extended droplet size ranges with mostly 2 size fractions only and time periods of typically hours, yielding volume-weighted sample concentrations which can significantly blur existing concentration gradients (Moore et al., 2004a, and references therein; Ogren and Charlson, 1992). Despite such difficulties, observations of size-dependent solute concentrations are still important as available measurements especially for more than two size fractions are very sparse. In the present study, a 3-stage and a 5-stage collector were applied and the observed solute concentration size dependencies are discussed in section 3.4 in view of the above described existing knowledge.

2 Materials and methods

2.1 Cloud water sampling

Cloud water sampling took place on top of a 20 m high tower at Mt. Schmücke (Thuringia, Germany, 50°39'16.5" N, 10°46'8.5" E, 937 m asl) with several collectors. Bulk cloud water samples were collected into pre-cleaned plastic bottles using the Caltech Active Strand Cloud Water Collector Version 2 (CASCC2, Demoz et al., 1996), which has a 50% collection efficiency cut-off diameter (D_{50}) of 3.5 µm and collects droplets by inertial impaction on Teflon strands within the airflow through the instrument. To increase the collected volume of cloud water for chemical analyses, 4 individual instruments were run in parallel with a time resolution of one hour. After weighing for volume determination, the samples were pooled, aliquots for different chemical analyses were taken and aliquots as well as leftover samples were stored at -20°C until analysis. For size-resolved droplet sampling a 3-stage collector (Raja et al., 2008) with nominal D_{50} of 22, 16, and 4 µm for stages 1, 2, and 3, respectively, was used. This collector is basically a size-fractionating version of the CASCC, using Teflon strands/banks with different diameters and different spacing in the 3 stages. In addition, the CSU 5-stage collector (Moore et al., 2002) with nominal D_{50} of 30, 25, 15, 10, and 4 µm for stages 1 – 5 was operated. In contrast to the 3-stage, the 5-stage collector impacts droplets on flat surfaces downstream of jets with decreasing diameters for air acceleration (cascade impactor design). It has to be noted, that experimentally determined D_{50}s for this sampler differ somewhat from the nominal values and that, even though droplet separating characteristics have been improved over other existing multistage collectors, there is still considerable mixing of droplets of different sizes within each stage (Straub and Collett, 2002). Due to limitations of the lateral channel blower applied in this study, the 5-stage collector was operated about 10% below its nominal air flow rate of 2.0 $m^3 min^{-1}$, which likely had a modest effect on its collection characteristics and adds some uncertainty to the real cut-off diameters. Sample handling from the multistage collectors was the same as described for the bulk collectors. Before each cloud event, the samplers were cleaned by spraying deionised water into the inlet (bulk collectors) or taking apart the individual stages and rinsing all surfaces with deionised water (multistage collectors). Control samples were taken after the cleaning procedures by spraying deionised water into the samplers and handling the collected water in the same way as the real samples.

2.2 Interstitial and residual particle sampling

To complement the liquid cloud water samples, droplet residuals and interstitial particles were sampled downstream of a counter-flow virtual impactor (CVI) and an interstitial inlet (INT). The CVI/INT system was set up in a building next to the measurement tower with the inlets installed through a window at 15 m height, facing south-west direction (215°). Details of the setup can be found elsewhere (Mertes et al., 2005; Schwarzenböck et al., 2000). In brief, interstitial particles and gases are separated from cloud droplets in the CVI by a counter-flow air stream which allows only droplets larger 5 µm in diameter to enter the system. Inside the CVI the droplets are evaporated in particle-free and dry carrier air, resulting in the formation of dry residual particles consisting of non-volatile cloud water components. Volatile components can be expected to evaporate during the drying process. The INT inlet samples interstitial particles and gases by segregating droplets larger 5 µm. Downstream of INT and CVI, particles were sampled on quartz filters (MK 360, Munktell, Bärenstein, Germany, 47 mm for CVI, 24 mm for INT) with sampling durations typically varying between ca. 4 and 8 hours (some shorter and longer sampling events existed as well). Filters were stored at -20°C for later offline analysis. Online measurements of submicron particle composition were performed by two aerosol mass spectrometers (AMS, Aerodyne Research Inc., USA): a C-TOF-AMS for droplet residuals (CVI, 5 min time resolution) and a HR-TOF-AMS for non-activated particles (INT, 2.5 min time resolution). Details of the AMS measurements will be given in a forthcoming companion paper of this special issue (Schneider et al., in preparation).

2.3 Valley sites aerosol sampling

Next to the Schmücke in-cloud site, two more valley sites upwind and downwind of the Schmücke were installed during HCCT-2010 to characterise air masses before and after their passage through the clouds. Characterisation of incoming aerosol was performed at the upwind measurement site close to the village of Goldlauter (50°38'15"N, 10°45'14"E, 605 m asl). A full description of the instrumental setup will be given in a forthcoming companion paper of this special issue (Poulain et al., in preparation). In brief, a commercial monitor for aerosols and gases (MARGA 1S, Metrohm Applikon, The Netherlands) was used for continuous (1 h time resolution) determination of water-soluble inorganic trace gases and particulate ions. The MARGA operated at a sampling rate of 1 $m^3 h^{-1}$ and consisted of a PM_{10} inlet, a wet rotating denuder absorbing water-soluble gases into deionised water (10 ppm

H_2O_2 added as biocide), a steam jet aerosol collector to grow and collect aerosol particles, and 2 ion chromatography systems for online cation and anion analysis. Size-resolved particle sampling was performed using a 5-stage Berner impactor with D_{50}s of 0.05, 0.14, 0.42, 1.2, 3.5, and 10 µm and a sampling flow rate of 75 l min^{-1}. Data from the downwind site has not been used in the present contribution.

2.4 Cloud microphysical and meteorological parameters

Cloud liquid water content (LWC), droplet surface area (PSA), and effective droplet radius (R_{eff}) were measured continuously by a particle volume monitor (PVM-100, Gerber Scientific, USA), which was mounted on the roof of a building next to the measurement tower. Droplet number distributions were obtained from a forward-scattering spectrometer probe (FSSP-100, PMS Inc., Boulder, CO, USA), sitting on the top platform of the measurement tower. A Ceilometer (CHM15k, Jenoptik, Jena, Germany) was installed at the upwind site Goldlauter to derive cloud base heights (CBHs). Standard meteorological parameters (temperature, air pressure, relative humidity, wind direction, wind speed, global radiation, precipitation) were determined by automatic weather stations (Vantage Pro2, Davis Instruments Corp., Hayward, CA, USA) both at the upwind site (ca. 3 m above ground) and on the Schmücke measurement tower (ca. 22 m above ground).

2.5 Chemical analyses

Cloud water from the different samplers was filtered through 0.45 µm syringe filters (IC Acrodisc 13, Polyethersulfone membrane, Pall, Dreieich, Germany) and analysed for inorganic ions Cl^-, NO_3^-, SO_4^{2-},Na^+, NH_4^+, K^+, Mg^{2+}, and Ca^{2+} by ion chromatography (IC) with conductivity detection (ICS3000, Dionex, Dreieich, Germany). Cation separation was performed in a CS16 column (3 mm) applying a methanesulfonic acid eluent, while anions were separated using a KOH eluent in an AS18 column (2 mm). Inorganic ions from CVI and INT filters were determined by the same method after extraction in deionised water (Milli-Q, Millipore, Schwalbach, Germany) and filtration through a 0.45 µm syringe filter. Blank correction of filter data took place by substracting mean concentrations from three unloaded field blank filters.

Dissolved organic carbon (DOC) was determined from filtered cloud water samples using a TOC-V_{CPH} analyser (Shimadzu, Japan) in the NPOC (non-purgeable organic carbon) mode

(van Pinxteren et al., 2009). Hydrogen peroxide (H_2O_2) in solution was determined (in sum with organic peroxides) by fluorescence spectroscopy (Shimadzu RF-1501) following the method of Lazrus et al. (1985). To stabilize peroxides during sample storage, p-hydroxyphenylacetic acid solution (POPHA) was added to aliquots of cloud water immediately after sampling to form a stable dimer (Rao and Collett, 1995). S(IV) and its reservoir species hydroxymethanesulphonate (HMS) were determined spectrophotometrically (Lambda 900, Perkin Elmer, Waltham, MA, USA) by the pararosaniline method (Dasgupta et al., 1980). Preservation of total S(IV) and HMS took place following the procedure described by Rao and Collett (1995). Concentrations of reactive compounds at the time of sample preservation can be biased due to reactions during the collection period. The extent of such artefacts will depend on reactant concentrations and cloud water pH and cannot easily be estimated. Cloud water pH was measured immediately after sampling using an MI-410 combination micro-electrode (Microelectrodes, Inc., USA) regularly calibrated at pH 4 and 7.

2.6 Data processing and back-trajectory analysis

Cloud water data are presented either as solute concentration ($\mu mol\ L^{-1}$ or $mg\ L^{-1}$) or as CWLs (sometimes also referred to as equivalent air concentrations) in $\mu g\ m^{-3}$. CWLs are derived from the solute concentrations by multiplication with the cloud LWC (in $g\ m^{-3}$) and the molar mass of the compound (in $g\ mol^{-1}$), where necessary. For comparison of CWLs between different instruments and/or sites, concentrations were normalised to standard temperature and pressure (STP: 273 K, 1013 mbar). Ambient temperature during the time of sampling was used for normalising cloud water collector data, while room temperature was used for CVI/INT, MARGA, and AMS data (room temp. at time of calibration for the ladder one). The open-source statistical software R (R Core Team, 2015) including the ggplot2 package (Wickham, 2009) was used for data processing and plotting. Back trajectories were calculated using the PC version of the HYSPLIT model (Draxler and Rolph, 2003) with GDAS 1° resolution data from NOAA's Air Resource Laboratory (http://ready.arl.noaa.gov/archives.php). Residence times indices (RTIs) for different land cover classes (water, natural vegetation, agriculture, urban areas, bare areas) were derived as proxies for the impacts of typical emissions over these areas on the sampled air masses following the methodology described by van Pinxteren et al. (2010).

3 Results and discussion

3.1 Cloud events

Within about 1/3 of the 6 weeks HCCT-2010 campaign Mt. Schmücke was covered in clouds. Based on the project philosophy of studying aerosol cloud interactions in a Lagrange-type approach, only those clouds were sampled for which local meteorological parameters (mainly wind direction) indicated a good possibility of sampling representative air masses at all three campaign sites ("connected" air flow, see Tilgner et al., 2014) without substantial loss of material between the sites (non-precipitating clouds only). After the campaign, these events were thoroughly evaluated regarding the hypothesis of a connected air flow (Tilgner et al., 2014), leading to the so-called "Full Cloud Events" (FCEs) with conditions appropriate to compare data from the different sites in a meaningful way. In Table 1 a list of the FCEs with cloud water samples available is given together with some additional information on meteorological and cloud microphysical conditions. Note that the numbering of the events is based on all clouds occurring during HCCT-2010 and is thus non-consecutive. A total of 8 FCEs were sampled, out of which some belonged to the same cloud appearance at Mt. Schmücke, but were interrupted either by rain or wind direction out of a predefined South-West corridor (FCE11.2+3 and FCE26.1+2). Two relatively long FCEs occurred with durations of 15 h, while the other events were shorter with 2 – 7 h durations. Mean LWCs ranged between 0.15 and 0.37 g m^{-3} and were a function of the in-cloud height of the measurement site (i.e. Schmücke above cloud base, derived from upwind site cloud base height measurements). Droplet surface areas were 700 – 1400 cm^2 m^{-3} on average with effective droplet radii of about 6 – 9 µm. Mean event temperatures decreased from about 9 °C for the first FCE to 1 – 2 °C for the last events at the end of the campaign . The numbers of samples for the different instruments are given in Table 1 as well according to the time resolutions of the samplers. Overall, meteorological and cloud microphysical conditions were typical for clouds at Mt. Schmücke during this time of the year. Many more details on meteorology are given in Tilgner et al. (2014).

3.2 Control samples and collector intercomparison

To check for possible contamination, control samples were taken from the cloud water collectors in between cloud events (section 2.1) indicating a "field blank" value for the species determined. Concentration levels in these blanks showed clear differences among the

three samplers with highest values from the CASCC2 bulk sampler (Figure S1). In contrast to the two multistage collectors, the CASCC2 was not disassembled for cleaning, which indicates that the cleaning procedure applied here (spraying deionised water through the sampler) is less effective in removing leftover traces from previously sampled cloud water (or its dried residuals if cleaning was not performed directly after the end of the event). Mean concentration levels in the controls are usually <10% of cloud water concentrations for more abundant ions (ammonium, nitrate, sulfate), but can make up significant fractions (up to 100% or even more in individual samples with low concentration) for trace ions (Figure S2). Mean blank levels of H_2O_2 and DOC are 25 and 15% of cloud water concentrations on average, respectively (Figure S2). The amount of carry-over contamination in the controls depends on concentration levels in the previous sample as well as on the effectiveness of the cleaning procedure (water volume applied, dried surfaces, etc.) and will likely vary from one event to another, which hampers a correction of cloud water concentrations by the available blank data. Carry-over contamination will likely affect the first sample of a new cloud event mainly, as the inside-surfaces of the CASCC2 are continuously washed by cloud water during operation and any contamination can be expected to be removed after the first hour of sampling. In addition, a fraction of the control sample concentrations can be suspected to form by uptake of gases during control sampling for species like ammonium (from ammonia), nitrate (from nitric acid), DOC (from water-soluble volatile organic compounds, VOCs), and especially H_2O_2. Cloud water concentrations are thus reported as measured in the following.

Comparisons of volume-weighted mean concentrations from the multistage collectors with bulk concentrations from the CASCC2 for main cloud water constituents (sulfate, nitrate, ammonium, DOC) are shown in Figure S3 and Figure S4. They reveal generally similar data between the samplers with a tendency of sometimes higher concentrations from the multistage collectors, which was, however, not consistently observed for all constituents and/or cloud events.

3.3 Bulk concentrations

3.3.1 Composition overview

In Table 2 concentrations of inorganic ions, H_2O_2 (aq), S(IV), HMS, and DOC as well as cloud water pH are summarised for the events given in Table 1. The observed range of pH-values was from 3.6 to 5.3, with a mean of 4.3. Highest ion concentrations (on a molar basis)

were observed for ammonium, followed by nitrate. Sulfate, chloride, and sodium showed considerably lower concentrations, while potassium, magnesium, and calcium were lowest. Arithmetic mean concentrations of this study are compared to literature data from clouds/fogs at other European sites in Table 3. Note that some authors report arithmetic means, while others report volume-weighted mean concentrations, which are always lower for a given dataset (see Table 2). Comparability of literature pH data is even more hampered as it is either reported as arithmetic mean or derived from either arithmetic or volume-weighted mean H^+ concentrations (the first approach leading to higher values than the other ones). In general, however, concentration levels in the present study are often similar to those observed in more recent campaigns at Puy de Dôme (continental non-polluted regime, Deguillaume et al., 2014), in the Western Sudety Mountains (Blas et al., 2008), and at the Schmücke site in a previous campaign (Brüggemann et al., 2005). In contrast, data from the 1980s and 1990s often show much higher concentrations of sulfate and nitrate (Bridges et al., 2002; Herckes et al., 2002; Wrzesinsky and Klemm, 2000; Acker et al., 1998; Joos and Baltensperger, 1991; Lammel and Metzig, 1991), presumably due to the decline in European emissions of NO_x and SO_2 over the past decades (EEA, 2014). Concentrations of DOC are more sparsely available in the literature for European clouds. Mean values during HCCT-2010 compare well with data from Puy de Dôme (continental non-polluted regime, Deguillaume et al., 2014), Rax (Löflund et al., 2002) and Schmücke (Brüggemann et al., 2005). Data for H_2O_2(aq) and S(IV) are even more sparse. In the present study, H_2O_2(aq) has been found to be within the same order of magnitude as determined in similar environments (Deguillaume et al., 2014; Brüggemann et al., 2005; Löflund et al., 2002), while S(IV) is at the lower end of reported concentrations.

Average relative compositions based on volume-weighted mean concentrations (in mg L^{-1}) are shown in Figure 1 for the main cloud events. DOC was converted to DOM (dissolved organic matter) using a conversion factor of 1.8 as in previous studies (Giulianelli et al., 2014; Benedict et al., 2012; Straub et al., 2012; Collett et al., 2008). Solute concentrations are always dominated by the main ions sulfate, nitrate, and ammonium, explaining approx. 60-70 % of total determined concentrations (campaign average 62 %). Among them, nitrate represents the dominant species (approx. 30-50 % of total concentrations, average 35 %), while sulfate and ammonium comprise lower fractions of total solutes (averages of 14 and 13 %, respectively). Organic compounds contribute approx. 20-40 % (average 28 %) and are thus another main constituent of cloud water dissolved material. These fractions are similar to what has been reported for background and anthropogenic influenced conditions at Puy de

Dôme (Marinoni et al., 2004) and are – despite the different environment – strikingly similar to the 20-year mean composition of Po valley fogs with 35 %, 15 %, 18 %, and 25 % contributions of nitrate, sulfate, ammonium, and DOM, respectively (Giulianelli et al., 2014).

The ion balance of inorganic anions versus cations (including $[H^+]$) is shown in Figure 2. An anion deficit is observed for nearly all samples, ranging up to 178 µeq L^{-1}. Inorganic anions missing from the calculation are unlikely to explain the deficit, as they will have a small impact on the ion balance only (bicarbonate < 1 µM for given pH values, bisulfite < 3.2 µM based on S(IV) and HMS data). Concentrations of a large number of organic acids were measured from the bulk cloud water samples and will be presented elsewhere (van Pinxteren et al., in preparation). Summing up the equivalent concentrations of the most abundant determined acids (formic, acetic, glycolic, oxalic, malonic, succinic, and malic acid) with consideration of their respective dissociation states depending on their pK_a values and sample pH values gives a range of 5 – 82 (average of 23) µeq L^{-1}, which explains 6 – 100% (average of 56%) of the inorganic anion deficit. In about 10% of the samples organic acid equivalent concentrations significantly exceeded the anion deficit (up to 255%), likely related to measurement uncertainties and/or non-determined cations. Considering that the DOC fraction likely contains many more than the analytically resolved organic acids, it can be assumed that the missing anions are predominantly organic in nature and that organic acidic material had a non-negligible impact on the cloud water acidity during HCCT-2010. Similar observations have been made before in other cloud/fog systems (Straub et al., 2012; Hegg et al., 2002; Khwaja, 1995; Collett et al., 1989).

3.3.2 Factors controlling solute concentrations

In Figure 3a the variability of observed solute concentrations for selected ions is indicated in box-plots. Variability was high both within events (max/min ratios of up to 5-8 for main ions during the longer events, and up to 5-34 for minor ions), as well as in-between events (max/min ratios of median conc. between 3 and 6 for main ions, 6-29 for minor ions). In general, cloud water solute concentration variability can be caused by i) changes in microphysical cloud conditions, e.g. supersaturation and LWC, ii) changes in CCN concentration, size distribution, and chemical composition, iii) changes in gas-phase concentrations of soluble gases and corresponding phase equilibria, and iv) chemical reactions

in the cloud water. Distinctly different concentration patterns can be observed in Figure 3a for three ion groups from similar sources, i.e. secondary ions ammonium, nitrate, and sulfate, sea-salt ions sodium and chloride, and the biomass burning and/or soil marker potassium, indicating a dominant influence of air mass history and thus CCN concentration and composition on cloud water solute concentrations. This is most obvious for sodium and chloride, which show highest concentrations during FCEs 1.1, 22.1, and 26.1+2. During these events, back-trajectory analysis revealed a stronger influence of marine emissions (residence time indices above water surfaces were between 0.3 and 0.5, as compared to < 0.2 for the remaining events, cf. Figure S5).

To remove any influence of LWC fluctuations, CWLs are plotted in Figure 3b. The CWL patterns resemble those of solute concentrations to a large extent, suggesting that for our dataset CCN composition and concentrations of soluble gases (i.e. air mass history) have a stronger impact on cloud water solute concentrations than LWC variability. Relative standard deviations (RSDs) of solute concentrations (whole campaign) are 66 %, 60 %, and 60 % for sulfate, nitrate, and ammonium, respectively, and 84-125% for trace ions. RSDs of CWLs are similar, sometimes even higher, with values of 80 %, 52 %, and 66 % for sulfate, nitrate, and ammonium, respectively, and 62-96 % for trace ions. Removing LWC variability, thus, does not reduce concentration variability, at least for the LWC range in this study. This is similar to observations of Aleksic and Dukett (2010) from a much larger dataset and indicates that LWC is obviously an important, but not necessarily the primary control factor of solute concentrations..

If at all, an inverse functional relationship between solute concentration and LWC (Elbert et al., 2000; Möller et al., 1996) can only be observed during single events (i.e. when CCN concentration and composition as well as gas phase concentrations might be regarded comparably constant) in our dataset. This is shown in Figure 4a for TIC versus LWC where the color-coded single event data indicates more or less constantly decreasing TIC with increasing LWC for some events. Overall, however, the pattern approximates those observed for larger datasets (Aleksic and Dukett, 2010; Kasper-Giebl, 2002; Möller et al., 1996): Maximum TICs are decreasing, while minimum TICs stay relatively constant with increasing LWC, leading to a range of observed TICs at any given LWC. As one and the same LWC value can result from different cloud microphysical conditions (e.g. few large drops vs. more small drops) and clouds with similar LWC can form in very different air masses, this is

actually an expected observation. In several other cloud/fog studies relationships between TIC and/or solute concentrations with LWC were reported to be non-existent, neither (Giulianelli et al., 2014; Straub et al., 2012; Marinoni et al., 2004; Kasper-Giebl, 2002).

The reason for this ostensible contradiction to the conclusions of the studies by Möller et al. (1996) and Elbert et al. (2000) might lie in different assessments of the quality of fitted models. Möller et al. (1996) and Elbert et al. (2000) report power law fits with coefficients of determination (R^2) of 0.27 and 0.38, respectively. Even when considering these values satisfactory (on the general usefulness of R^2 especially for goodness-of-fit of nonlinear models see Spiess and Neumeyer (2010)), the presented scatter plots leave room for questioning the ability of the fitted functions to adequately represent the data.

Instead of LWC, Marinoni et al. (2004) report TIC in cloud water at Puy de Dôme to be a power function of effective droplet radius (R_{eff}), even though with similarly poor R^2 of 0.29. In Figure 4b, TIC during HCCT-2010 is plotted against R_{eff}, which was determined by the PVM as well. In contrast to LWC, both maximum and minimum TIC values are decreasing with increasing R_{eff} in this plot and the relationship comes indeed closer to a functional one (best fit for simple linear regression; R^2 increases from 0.14 with LWC to 0.52 with R_{eff} as explanatory variable). There is, however, still substantial unexplained TIC variation, likely arising from different broadness and/or skewness of the droplet size spectrum and from processes like phase equilibria and/or aqueous phase reactions.

In Figure 4c and Figure 4d the relationships of DOC with LWC and R_{eff} are shown, which are very similar to the ones observed for TIC. Herckes et al. (2013) examine total organic carbon (TOC) concentrations against LWC for a number of different sites worldwide. A simple relationship explaining the variation across all locations could not be identified by the authors. However, their plot looks remarkably similar to the plots of TIC vs. LWC from the larger datasets referenced above (decreasing spread of concentrations with increasing LWC), indicating that the main factors controlling the organic content of fog and cloud water are the same as the ones determining inorganic ion concentrations (likely nucleation scavenging and some additional gas phase uptake).

As a further means to study the various influences on solute concentrations, principal component analysis (PCA) was performed on cloud water solute concentrations and pH, back trajectory RTIs, LWC, and R_{eff}. Factor loadings of 4 extracted principal components after Varimax rotation are shown in Table 4. The first factor is highly correlated to air mass

residence times above the oceans and cloud water concentrations of sea-salt constituents sodium, magnesium, and chloride. The second factor shows high loadings for all 4 main cloud water solutes (sulfate, nitrate, ammonium, DOC), representing typical main particulate components in aged continental air masses. The third factor is highly correlated to potassium and calcium concentrations and air mass residence times above agricultural lands and likely represents a mixed soil/biomass burning influence. The fourth factor mainly includes the variability of air mass residence times above urban areas, with no strong correlation to cloud water constituents. pH shows a weak anticorrelation to this factor, which could indicate an impact of acidic pollutants in comparably fresh air masses.

LWC has a much smaller impact on the marine factor than air mass residence time above water and its loading on factor 2 is weak as well (in contrast to R_{eff}, which has a significant impact on this factor). This further supports the conclusion of LWC variability impacting solute concentrations to a lesser extent if several clouds with different air mass histories are considered.

In summary, the discussion in this section shows that no single factor is available to adequately describe the complex processes controlling solute concentrations of both inorganic and organic material in bulk cloud water. If a simple functional relationship is needed, R_{eff} might be a somewhat better choice than LWC. The probabilistic approach of Aleksic, however, seems more appropriate: For any given LWC (and probably R_{eff} as well), solute concentrations exhibit a (non-linear) distribution, as they depend on several other variables at the same time.

3.3.3 Comparison of bulk vs. CVI concentrations

In parallel to the bulk cloud water sampling, a CVI separated droplets from the interstitial phase and enabled the chemical characterisation of residual particles from filters and online with an AMS (section 2.2). The resulting CWLs of main solutes (normalised to standard conditions) are compared to the ones obtained from bulk cloud water samples in Figure 5. As can be seen, the temporal trends are often similar from both time-resolving samplers (CASCC2 and CVI-AMS), while absolute values can differ. During FCEs 11.3, 22.1, and 26.1+2, the ratios between CASCC2 and CVI-AMS CWLs are close to 1, especially for ammonium and sulfate (see Figure S6 for ranges of CWL ratios). During FCEs 1.1, 11.2, and 13.3, this ratio is close to 2 (median), while it can be even higher for nitrate. Time-integrated

mean CWLs from CVI filters are mostly close to the values from the CVI-AMS for sulfate and nitrate (with the exception of FCE1.1), while for ammonium, they are substantially lower during 4 out of the 6 events shown. CWL deviations for DOC (for residual particle data calculated as AMS organics divided by a conversion factor of 1.8 as above) tend to be lower than for the ions and CASCC2/CVI-AMS ratios are even below 1 during FCEs 1.1, 11.2, and 26.1+2 (Figure S6). DOC CWLs from CVI filters are not given due to unreliable data from the small masses sampled on the filters.

Possible reasons for these deviations are manifold and include i) different sampling locations in the cloud (tower versus inlet at house wall), ii) different cut-off and detection characteristics (all dissolved bulk material analysed from CASCC2, while AMS measures non-refractory submicron residual particles only), iii) different assumptions/corrections for sampling efficiency (assumption of constant sampling efficiency across droplet size spectrum for CASCC2, correction of CVI sampling efficiencies based on particle number size distributions), iv) measurement uncertainties of analytical methods, AMS, and PVM for LWC measurement, v) – for DOC – uncertainty in the OM to OC conversion factor (1.8) and inclusion of undissolved organic matter in the AMS residual organics concentration, vi) – for filter samples – potential negative artifacts from evaporation of semi-volatile particle constituents during sampling as well as uncertainty from blank correction especially for short sampling times and low sampled masses, and vii) – very important for some species - different droplet "pretreatment", i.e. liquid collection in the bulk sampler versus evaporation of water and volatile constituents such as ammonia, nitric acid and dissolved VOCs in the CVI. Given all these uncertainties and systematic differences, a general agreement between CWLs obtained from the different samplers within a factor of 2 appears well acceptable. A notable exception with much less agreement is nitrate during FCE11.2, where bulk cloud water CWLs are about a factor of 3.5 higher than CVI concentrations. The reason for the large deviation during this event is likely an enhanced concentration of nitric acid, which is taken up as nitrate into the bulk cloud water, but can be (partly) released back to the gas phase during droplet drying in the CVI (see also the following section).

3.3.4 Scavenging efficiencies

Scavenging efficiencies (SEs) were calculated by two different approaches. "In-cloud SEs" are based on cloud water loadings and interstitial particle concentrations (both being normalised to STP) and are calculated as follows:

$$SE_{in-cloud} = \frac{CWL}{CWL + c_{int}} \quad \text{(Equation 1)}$$

with $SE_{in-cloud}$: in-cloud scavenging efficiency

CWL: cloud water loading in µg m^{-3}, either from bulk cloud water (CASCC2) or from droplet residual concentrations (CVI-AMS and CVI-Filter)

c_{int}: interstitial particle concentration in µg m^{-3} (INT-AMS or INT-Filter)

"Upwind SEs", in contrast, are based on a comparison of STP normalised CWLs and upwind concentrations, calculated as:

$$SE_{upwind} = \frac{CWL}{c_{upw}} \quad \text{(Equation 2)}$$

with SE_{upwind}: upwind scavenging efficiency

CWL: cloud water loading in µg m^{-3} from bulk cloud water (CASCC2)

c_{upw}: upwind concentration from MARGA measurements in µg m^{-3}, either particulate only or total aerosol (particulate + gaseous concentration)

The results of these calculations are shown in Figure 6. In-cloud SEs calculated from the different samplers usually agree well except for cases where sampler intercomparison was poor (section 3.3.3). Comparison with upwind SEs, however, reveals substantial differences, which are summarised as event means in Table 5 (for residual in-cloud SEs only the ones based on CVI/INT AMS data are given here to avoid redundancy). Mean in-cloud SEs for sulfate are usually >= 0.9 except for FCE11.2 and FCE13.3, where substantial fractions (21-44%, depending on data used) of in-cloud sulfate reside in interstitial particles. During these events particle activation curves obtained from comparing measured particle number size distributions upwind and in-cloud were comparably shallow and the critical activation diameter was larger than during other events (Figure S7), consistent with larger fractions of submicron sulfate not being activated to cloud droplets due to cloud microphysical conditions. Consistent with our data, in-cloud SEs of sulfate between 0.52 and 0.99 have been reported for clouds at Puy de Dôme, Brocken, and Mt. Sonnblick (Sellegri, 2003; Acker et al., 2002; Hitzenberger et al., 2000; Kasper-Giebl et al., 2000), with larger values being more typical.

In contrast to in-cloud SEs, sulfate upwind SEs were mostly << 0.9, indicating incomplete mass conservation between the sites. From previous studies at the Schmücke (Brüggemann et al., 2005; Herrmann et al., 2005) and results on aerosol processing presented in a forthcoming

companion paper, it is known that various physical loss processes, such as scavenging of cloud droplets by trees and/or entrainment of cleaner air masses from aloft can reduce observed concentrations of all particle constituents along the air path from upwind via Schmücke towards the downwind site. Upwind SEs being smaller than in-cloud SEs support these conclusions of physical particulate mass losses from the upwind to the in-cloud site. Only during FCE13.3 upwind SEs are found to be higher than in-cloud SEs, indicating additional sulfate mass within the cloud, which could result from chemical production, uptake of gaseous H_2SO_4 (Roth et al., 2016; Harris et al., 2014; Harris et al., 2013) and/or other processes (e.g. entrainment). Similar to sulfate, ammonium shows in-cloud SEs typically > 0.9, except for FCE13.3 (large activation diameter). Upwind SEs are similarly large if upwind particulate ammonium concentrations are considered only, but drop to mean values between 0.4 and 0.7 if gaseous upwind ammonia - which is likely to be taken up by the cloud water at least partially- is included in the balance. Consistent with the conclusions from sulfate, the lower overall upwind SEs thus likely reflect the impact of physical loss processes at the sites.

For nitrate and DOC, these comparisons look different. While in-cloud SEs are again > 0.9 in most cases, upwind SEs are > 1 in most cases, indicating additional nitrate and DOC at the in-cloud site (note that event mean DOC upwind SEs in Table 5 were calculated using water-soluble organic carbon concentrations from impactor samples, as the MARGA analyses inorganic ions only). For DOC, this most likely results from uptake of water-soluble VOCs (e.g. acids, aldehydes, ketones) into cloud droplets. The highest value was observed for FCE11.2, where the inorganic anion deficit was highest as well (Figure 2), indicating that a significant amount of organic material taken up from the gas-phase must have been acidic or – alternatively – neutral compounds were oxidised to organic acids upon dissolution in the cloud droplets. It is noted that the main organic acids mentioned above explain only less than 10% of the inorganic anion deficit for this event.

For nitrate, upwind SEs stay similarly high or even higher than in-cloud SEs even after considering any upwind HNO_3 measured by the MARGA. Especially when considering that nitrate likely experiences similar physical mass losses as ammonium and sulfate (which typically were on the order of 10 – 40% at the downwind site, data not shown here), this would imply a nitrate budget at the cloud site substantially larger than the sum of particulate and gaseous nitrate at the upwind site. Given that aqueous phase oxidation of NO_x to nitrate can be considered negligible (Seinfeld and Pandis, 2006) and a potential positive nitrate

595 artefact from hydrolysis of N_2O_5 in the cloud water can be assumed to be present in similar
596 magnitude in the wet rotating denuder samples of the MARGA system (Phillips et al., 2013),
597 such a large budget increase of nitrate at the cloud site seems unrealistic. In addition, a
598 comprehensive data analysis focussing on aerosol processing during FCEs (manuscript in
599 preparation) does not yield indications for increased nitrate at a site downwind of the cloud,
600 neither on average over all FCEs, nor specifically during FCE11.2, where nitrate enrichment
601 was highest. Any additional nitrate in the cloud water thus needs to evaporate back to the gas
602 phase upon cloud dissipation.

603 The most likely explanation for the observed discrepancy is a severe underestimation of nitric
604 acid by the MARGA system. Accurate nitric acid determination is known to be challenging
605 due to the "stickiness" of the molecule (Rumsey et al., 2014) and adsorption in the inlet was
606 reported to be strongly increased when sampling air – as during FCE sampling - is near 100%
607 RH (Neuman et al., 1999). As the inlet HDPE tubing during HCCT-2010 was approx. 3.5 m
608 long (from PM_{10} head to denuder), significant losses of HNO_3 before denuder sampling seem
609 likely. In a not (yet) published intercomparison of nitric acid between the MARGA unit as
610 used during HCCT-2010 and a separate batch denuder with inlet tubing reduced to a
611 minimum, concentration ratios between the MARGA and the reference denuder were
612 typically between 0.17 and 0.98 (10^{th} and 90^{th} percentile, G. Spindler and B. Stieger, personal
613 communication). Using a value of 0.25 (lower quartile of the intercomparison) as a correction
614 factor for nitric acid measured during HCCT-2010 (i.e. multiplying measured apparent
615 concentrations by 4) yields upwind SEs for total nitrate between 0.7 and 1.2 (as event means),
616 which would be more consistent with the values obtained for ammonium and sulfate.

617 An enrichment of cloud water nitrate has previously been observed in several studies and has
618 usually been related to the uptake of nitric acid as the most probable explanation (Prabhakar
619 et al., 2014; Hayden et al., 2008; Brüggemann et al., 2005; Sellegri et al., 2003; Cape et al.,
620 1997), which is in agreement with our considerations described above.

621 In conclusion, the comparison of upwind and in-cloud scavenging efficiencies reveals that i)
622 nucleation scavenging typically removed >80 %, often close to 100 % of soluble material
623 from the particle phase upon cloud formation, ii) uptake of gaseous ammonia, nitric acid and
624 water-soluble VOCs had an additional significant impact on observed cloud water
625 concentrations, and iii) particulate material is clearly lost or diluted to some extent between

626 the upwind and the in-cloud site, likely due to physical processes such as droplet scavenging
627 by trees and/or entrainment of cleaner air masses.

628

629 ## 3.4 Size-resolved droplet compositions

630 ### 3.4.1 3-stage collector

631 In Figure 7 volume-weighted mean (VWM) concentrations per cloud event are shown for
632 ions, H_2O_2, and DOC within the droplet size classes of the 3-stage collector. Even though the
633 nominal cut-off diameters of the 3 stages are given in Figure 7, it has to be noted, that in
634 reality significant mixing of droplets between the nominal size classes occurs due to the
635 relatively broad collection efficiency curves (Straub and Collett, 2002). Concentrations in a
636 given droplet size class are thus influenced by droplets from other size classes to a significant
637 extent and the size distributions can only reflect an approximate picture of the real pattern.
638 Volumes of cloud water collected per stage were between 5.9 and 240 ml with typically
639 lowest volumes on the intermediate stage (16-22 µm) and highest volumes in the smaller or
640 larger size class, depending on the sample (see Figure S8 for details).

641 Volume-weighted mean concentrations per event were calculated to reduce the complexity of
642 the data set, even though information on the temporal evolution of size-resolved
643 concentrations is lost by the averaging. Data for all individual samples taken with the 3-stage
644 collector is given in the Supplemental Material (Figure S9 – Figure S18). As can be seen
645 there, concentrations levels of individual cloud water constituents can vary significantly
646 within one cloud event while the general patterns of concentrations in the three droplet size
647 classes are often quite persistent during an event (exceptions will be noted below). For the
648 major ions sulfate, nitrate, and ammonium, two main profiles of size-resolved cloud water
649 concentrations can be observed in the VWM data: i) decreasing concentrations with
650 increasing drop size for FCEs 1.1, 11.2, 11.3, 13.3, and ii) profiles with minimum
651 concentrations in medium-sized droplets on stage 2 ("U"-shaped profiles) for FCEs 22.1 and
652 FCE26.1+2. Only for nitrate during FCE1.1 a profile of increasing concentrations with
653 increasing drop size is observed. Concentration differences between highest and lowest values
654 are usually within a factor of 2 with the exception of FCE11.2, where concentrations of
655 sulfate and ammonium in large drops were a factor of 3-4 lower than in small drops (on
656 VWM basis). The two types of profiles reflect the dominant profiles of major ions in the

657 individual samples (Figures S9 – Figure S11) for most of the events. Only during FCE1.1 and
658 mainly for sulfate and ammonium, the VWM profile does not adequately represent the
659 individual profiles, which were rather variable during the first half of this 15h event and
660 stabilized to a profile of increasing concentrations with increasing drop size during the second
661 half of the event. As sampled water volumes were comparably low during the second half of
662 the event, however, their weight to the volume-weighted mean profile is rather low. Literature
663 data from 3-stage cloud water collectors is very sparse. Raja et al. (2008) report decreasing
664 concentrations of main ions with increasing drop size for fog samples in the US Gulf coast
665 region, obtained with the same collector as in the present study. Collett et al. (1995) observed
666 U-type profiles in cloud samples obtained with a different 3-stage collector (different nominal
667 cut-offs) from two sites in North Carolina and California, USA.

668 The VWM profiles of low concentration ions (chloride, sodium, magnesium, calcium, and –
669 in part – potassium) were found to be markedly different from the major ion profiles.
670 Concentrations were usually increasing with increasing drop size, especially for events with
671 elevated concentrations (FCE1.1, 22.1, and 26.1+2) due to elevated impact of marine
672 emissions on sampled air masses (cf. section 3.3.2). Also, observed concentration differences
673 in different drop size ranges tended to be larger (up to a factor of 10) as compared to major
674 ion concentrations. Available literature data for minor ions in three drop size ranges reveals
675 diverse profiles, depending on species and location (Raja et al., 2009; Collett et al., 1995).

676 In contrast to the ionic data, concentrations of H_2O_2 in different collector stages were
677 comparably homogeneous, with maximum differences of 25% (or a factor of 1.3). This is
678 likely related to the different incorporation pathway (uptake from gas-phase as compared to
679 nucleation scavenging for the ions), which is expected to yield more similar concentrations in
680 differently sized cloud drops, at least if equilibrium conditions are assumed (Hoag et al.,
681 1999).

682 Both uptake pathways can in principle occur for DOC (VOC uptake and/or dissolution of
683 CCN organic material). The size-resolved concentration pattern in Figure 7, however,
684 resembles those of major ions, suggesting nucleation scavenging as the major path of DOC
685 incorporation into cloud water during this study.

686 Mean pH values per event (based on VWM concentrations of H^+) are shown in Figure 8a. A
687 similar pattern of slightly (approx. 0.1 pH units per stage) increasing values with increasing
688 drop diameter can be observed for nearly all events and collector stages. In individual samples

689 (Figure S19) differences between stages can be somewhat higher (up to approx. 0.5 pH units),
690 but the general patterns look similar to the VWM event averages. Qualitatively, increasing pH
691 with drop size is consistent with i) coarse (and typically less acidic) CCNs leading to larger
692 droplets (cf. elevated concentrations of coarse particle mode constituents), and ii) reduced
693 (diluted) concentrations of potentially acidic constituents (sulfate, nitrate, DOC) in larger
694 drops (Collett et al., 1994).

695 These observations highlight the complexity of solute concentration drop size dependencies.
696 Even for the comparably uniform conditions of the present study (same site, same season,
697 similar air mass origins, similar heights within the cloud), different profiles can result for one
698 and the same ion. This becomes even more obvious from individual samples (e.g. sulfate
699 during FCE1.1, Figure S9), where – as stated above – a number of different profiles can occur
700 during the same cloud event. Considering that these individual samples represent volume-
701 weighted averages over 2 hours, it is easy to imagine that with a higher time resolution of
702 sampling the variability of observed profiles would even increase. Without detailed numerical
703 modelling (which is beyond the scope of this study), a quantitative understanding of these
704 profiles and their variations seems impossible. In addition, the sampler characteristics (few
705 stages with broad collection efficiencies) together with changing droplet size distributions in a
706 cloud might influence the observed size dependencies. Even though drop volume size
707 distributions were usually similar both between events (Figure S20) and between individual
708 samples within the events (Figure S21), subtle changes, e.g. in the broadness of the
709 distribution or in the abundance of large (> 30 µm) drops, can – together with the broad
710 mixing of differently sized drops – lead to artificial modifications in the observed volume-
711 weighted concentrations on the three stages (Moore et al., 2004a). Despite these difficulties,
712 two broad conclusions from the 3-stage sf-CASCC ion data can be drawn: (i) main ions
713 (sulfate, nitrate, ammonium) have similar solute concentration drop size dependencies
714 (consistent with their presumed strong internal mixing in CCNs) and are often enriched in
715 smaller sized droplets (even though other, especially U-type profiles do occur as well), and
716 (ii) increasing concentrations with increasing droplet sizes, which might be expected based on
717 the consideration of the simple Ogren et al. (1992) model (see section 1), are mainly
718 observed if a strong coarse mode in upwind particles is present for a given constituent (e.g.
719 for sodium, magnesium, chloride, and nitrate- during FCE1.1; cf. Figure S22 and Figure S23
720 for size distributions of inorganic ions at upwind site during FCEs). These findings are
721 consistent with the availability of coarse CCN being an important prerequisite for such an

722 inverse concentration – size relationship to develop (Schell et al., 1997), although other
723 factors likely contribute to these observations as well.

724

725 ### 3.4.2 5-stage collector

726 Size-resolved concentrations of ions and H_2O_2 from the 5-stage collector are given in Figure 9
727 in the same way as described above for the 3-stage data (event VWM and normalised data).
728 Collected cloud water volumes were from 0.55 to 15 ml, with smallest volumes typically in
729 the 4-10 µm droplet size range and largest ones mostly for droplets >30 µm (see also Figure
730 S24). Concentration profiles of individual samples are shown in Figure S25 – Figure S33).
731 The number of events is smaller, as this sampler was not operated during FCE1.1 and
732 FCE26.1+2. Due to the relatively low volume of cloud water the 5-stage collector is
733 sampling, DOC analysis could not be performed from these samples. For major ions, the
734 patterns are broadly consistent with the profiles of decreasing concentrations with increasing
735 drop size observed from the 3-stage collector for FCEs 11.2, 11.3, and 13.3, with FCE22.1
736 showing some similarity to a U-shape (even though the concentration increase towards larger
737 drops is observable on stage 2 only, not on stage 1 collecting the largest drops). Concentration
738 differences between smallest and largest droplets are somewhat more pronounced (typically a
739 factor of about 2) as compared to the 3-stage collector (typically smaller than a factor of 2),
740 illustrating the higher efficiency of the 5-stage collector in separating small and large drop
741 populations. Sharpest concentration differences are usually observed between stage 4 and 5
742 (small droplets). This is true for basically all of the individual samples as well (Figure S25 –
743 Figure S33). Concentration patterns on stages 1-4, however, can vary somewhat within a
744 single event, depending on the development of the cloud. For example, nitrate shows
745 constantly decreasing concentrations with increasing drop sizes during the first half of
746 FCE11.2 (Figure S26), while during the second half, concentrations in larger drops tend to
747 increase. Similarly, ammonium concentrations develop from a maximum in medium-sized
748 drops for the first sample to notably homogeneous concentrations across all 5 collector stages
749 (difference of only about 30 % between smallest and larges drops) during FCE11.2 (Figure
750 S27). The observed profiles differ from those reported from a hill cap cloud at Whiteface,
751 NY, USA, using the same 5-stage collector (Moore et al., 2004a), where U-type profiles with
752 highest concentrations in largest drops were observed for ammonium and nitrate, while
753 sulfate showed increasing concentrations with increasing drop size through all 5 stages. The

same study reports 5-stage concentration profiles from a fog event in Davis, CA, USA, which are more similar to those in this study, with decreasing concentrations with increasing drop size (Moore et al., 2004a).

The patterns of trace ions also show some similarity with the ones observed from the 3-stage collector, mainly in that concentrations tend to increase from medium-sized towards larger droplets for most ions and events as well. There are, however, two distinct features in the 5-stage data which are not captured by the 3-stage collector: First, similar to the main ions, the concentration increase towards larger droplets is often (though not always) observable on stage 2 only, with decreasing concentrations on stage 1 (largest drops). Second, all trace ions show a very pronounced concentration increase in smallest droplets (stage 5), with often a factor of 5-10 difference to stage 4 concentrations, which is usually not seen in the 3-stage data, where smallest droplets are mixed with much larger ones on stage 3, leading to more diluted concentrations. Literature data on size-resolved trace ion concentrations from 5-stage collectors is available only for calcium, for which a pronounced U-type profile with highest concentrations in largest drops was reported (Moore et al., 2004a), while sodium, potassium and chloride ions were mentioned to have very similar profiles.

Compared to ionic content, the concentrations of H_2O_2 are more homogeneously distributed between the collector stages (maximum deviation < 50%) - similar to what was observed from the 3-stage collector data - and a general pattern cannot be observed from the (few) data available.

Event-averaged pH values from the 5-stage collector are given in Figure 8b (for individual samples in Figure S34). Highest values were mostly observed in smallest droplets (stage 5) with a significant decrease towards the next droplet size range (stage 4) at least during 3 out of the 4 events. From collector stage 4 towards stage 2 (increasing drop sizes) pH values tend to increase, similar to what is observed from the 3-stage collector (Figure 8a), while in largest drops (stage 1) they decrease again (to different extents). Overall, pH variations between different drop size classes are not too large for the sampled clouds with maximum differences of about 0.6 pH units on event-averaged basis.

These observations are generally consistent with the findings from the 3-stage collector. However, they also highlight the higher efficiency of drop population separation of the 5-stage collector as compared to the 3-stage collector, as ratios between minimum and maximum concentrations are larger and the sharp concentration increase towards the smallest

droplets (especially for trace ions) is only observed here (for volume size droplet distributions during 5-stage sampling see Figure S35). In addition, the observation of often decreasing concentrations from stage 2 (second-largest drops) to stage 1 (largest drops) might reflect the transition from region II (condensation growth) to region III (coalescence growth) in the Ogren et al. (1992) model (section 1), even though it must be noted that collection efficiency curves of these two stages are overlapping to a comparatively large extent (Straub and Collett, 2002). Compared to the study of Moore et al. (2004a) stressing the importance of cloud age (drop growth time) by comparing two different types of clouds/fogs, our data from more similar cloud systems highlights the impact of the size distributions of CCN constituents on the development of size-resolved concentration patterns. Both parameters were predicted to be relevant from detailed model sensitivity studies (section 1, Schell et al., 1997). In addition, despite the considerable mixing of droplets with different sizes occurring in the samplers, the data reveal the substantial differences which can exist in different droplet size classes as well as the variability of observed solute concentration profiles even under comparably similar cloud conditions. As such differences impact both chemical reactions in cloud drops and deposition efficiencies and can thus modify atmospheric sink and/or source strengths of PM constituents (Moore et al., 2004b), further observational and modelling studies on size-resolved droplet compositions seem important.

4 Conclusions

The analysis of bulk and size-resolved cloud water samples and related measurements of 8 cloud events during HCCT-2010 has led to the following main conclusions:

- Variability of solute concentrations in bulk samples was high for the clouds studied and was caused mainly by the variability of CCN concentrations and compositions, i.e. air mass history, in contrast to earlier suggestion of LWC generally being the main driver in solute concentration variation.
- A simple functional relationship between LWC and solute concentrations was observed only within single cloud events with little variation in incoming air mass concentrations and conditions. Across several events, no single factor is available to adequately describe the complex processes determining observed solute concentrations in cloud water. If a simple function is needed, R_{eff} might be a somewhat better choice than LWC.

- Both nucleation scavenging and gas-phase uptake contributed to observed cloud water concentrations of major constituents, with the first one being especially important for sulfate and the second one for nitrate.
- Losses of particulate mass occur from the upwind to the in-cloud site, observed from different in-cloud vs. upwind scavenging efficiencies and likely related to physical loss processes such as droplet scavenging and/or entrainment.
- Solute concentration droplet size profiles can be highly variable even within single events and were only partly consistent with considerations from a simple conceptual model. The observations made highlight the importance of CCN constituents' size distributions on the development of concentration profiles, consistent with earlier numerical simulation results.
- The comprehensive dataset obtained during HCCT-2010 will serve as a reference for the further development and evaluation of multiphase models in future studies.

Supplemental material related to this article is available online at doi: …

Acknowledgements

The authors acknowledge the support of several TROPOS staff members during cloud water sampling (even at unearthly hours), Jenoptik for providing the Ceilometer, the German Federal Environmental Agency (UBA) for providing the MARGA (contract 35101070) and the German Weather Service (DWD) and UBA for their cooperation and support at the Schmücke field site. HCCT-2010 was partially funded by the German Research Foundation (DFG) under contract HE 3086/15-1. The participation of Stephan Mertes was funded by the DFG priority program HALO (SPP 1294, grant HE 939/25-1). Partial additional support for Colorado State University was provided by the U.S. National Science Foundation (AGS-0711102 and AGS-1050052).

References

Acker, K., Möller, D., Marquardt, W., Brüggemann, E., Wieprecht, W., Auel, R., and Kalass, D.: Atmospheric research program for studying changing emission patterns after German unification, Atmos. Environ., 32, 3435-3443, doi: 10.1016/S1352-2310(98)00041-7, 1998.

Acker, K., Mertes, S., Moller, D., Wieprecht, W., Auel, R., and Kalass, D.: Case study of cloud physical and chemical processes in low clouds at Mt. Brocken, Atmos. Res., 64, 41-51, doi: 10.1016/S0169-8095(02)00078-9, 2002.

Aleksic, N., and Dukett, J. E.: Probabilistic relationship between liquid water content and ion concentrations in cloud water, Atmos. Res., 98, 400-405, doi: 10.1016/j.atmosres.2010.08.003, 2010.

Bator, A., and Collett, J. L.: Cloud chemistry varies with drop size, J. Geophys. Res. - Atmos., 102, 28071-28078, doi: 10.1029/97jd02306, 1997.

Benedict, K. B., Lee, T., and Collett, J. L.: Cloud water composition over the southeastern Pacific Ocean during the VOCALS regional experiment, Atmos. Environ., 46, 104-114, doi: 10.1016/j.atmosenv.2011.10.029, 2012.

Beswick, K. M., Choularton, T. W., Inglis, D. W. F., Dore, A. J., and Fowler, D.: Influences on long-term trends in ion concentration and deposition at Holme Moss, Atmos. Environ., 37, 1927-1940, doi: 10.1016/S1352-2310(03)00046-3, 2003.

Blas, M., Sobik, M., and Twarowski, R.: Changes of cloud water chemical composition in the Western Sudety Mountains, Poland, Atmos. Res., 87, 224-231, doi: 10.1016/j.atmosres.2007.11.004, 2008.

Brantner, B., Fierlinger, H., Puxbaum, H., and Berner, A.: Cloudwater Chemistry in the Subcooled Droplet Regime at Mount-Sonnblick (3106-M Asl, Salzburg, Austria), Water Air Soil Poll., 74, 363-384, 1994.

Bridges, K. S., Jickells, T. D., Davies, T. D., Zeman, Z., and Hunova, I.: Aerosol, precipitation and cloud water chemistry observations on the Czech Krusne Hory plateau adjacent to a heavily industrialised valley, Atmos. Environ., 36, 353-360, doi: 10.1016/S1352-2310(01)00388-0, 2002.

Brüggemann, E., Gnauk, T., Mertes, S., Acker, K., Auel, R., Wieprecht, W., Möller, D., Collett, J. L., Chang, H., Galgon, D., Chemnitzer, R., Rüd, C., Junek, R., Wiedensohler, W., and Herrmann, H.: Schmücke hill cap cloud and valley stations aerosol characterisation during FEBUKO (I): Particle size distribution, mass, and main components, Atmos. Environ., 39, 4291-4303, doi: 10.1016/j.atmosenv.2005.02.013, 2005.

Cape, J. N., Hargreaves, K. J., StoretonWest, R. L., Jones, B., Davies, T., Colvile, R. N., Gallagher, M. W., Choularton, T. W., Pahl, S., Berner, A., Kruisz, C., Bizjak, M., Laj, P., Facchini, M. C., Fuzzi, S., Arends, B. G., Acker, K., Wieprecht, W., Harrison, R. M., and Peak, J. D.: The budget of oxidised nitrogen species in orographic clouds, Atmos. Environ., 31, 2625-2636, doi: 10.1016/S1352-2310(96)00192-6, 1997.

Collett, J. L., Daube, B., Munger, J. W., and Hoffmann, M. R.: Cloud water chemistry in Sequoia National Park, Atmos. Environ., 23, 999-1007, 1989.

Collett, J. L., Bator, A., Rao, X., and Demoz, B. B.: Acidity Variations across the Cloud Drop Size Spectrum and Their Influence on Rates of Atmospheric Sulfate Production, Geophys. Res. Lett., 21, 2393-2396, doi: Doi 10.1029/94gl02480, 1994.

Collett, J. L., Iovinelli, R., and Demoz, B.: A three-stage cloud impactor for size-resolved measurement of cloud drop chemistry, Atmos. Environ., 29, 1145-1154, doi: 10.1016/1352-2310(94)00338-l, 1995.

893 Collett, J. L., Sherman, D. E., Moore, K. F., Hannigan, M. P., and Lee, T.: Aerosol particle
894 processing and removal by fogs: Observations in chemically heterogeneous central
895 California radiation fogs, Water Air Soil Poll.: Focus, 1, 303-312, 2001.

896 Collett, J. L., Herckes, P., Youngster, S., and Lee, T.: Processing of atmospheric organic
897 matter by California radiation fogs, Atmos. Res., 87, 232-241, doi:
898 10.1016/j.atmosres.2007.11.005, 2008.

899 Dasgupta, P. K., Decesare, K., and Ullrey, J. C.: Determination of Atmospheric Sulfur-
900 Dioxide without Tetrachloromercurate(Ii) and the Mechanism of the Schiff Reaction,
901 Anal. Chem., 52, 1912-1922, doi: 10.1021/Ac50062a031, 1980.

902 Daum, P. H., Kelly, T. J., Schwartz, S. E., and Newman, L.: Measurements of the Chemical
903 Composition of Stratiform Clouds, Atmos. Environ., 18, 2671-2684, doi:
904 10.1016/0004-6981(84)90332-9, 1984.

905 Deguillaume, L., Charbouillot, T., Joly, M., Vaïtilingom, M., Parazols, M., Marinoni, A.,
906 Amato, P., Delort, A. M., Vinatier, V., Flossmann, A., Chaumerliac, N., Pichon, J. M.,
907 Houdier, S., Laj, P., Sellegri, K., Colomb, A., Brigante, M., and Mailhot, G.:
908 Classification of clouds sampled at the puy de Dôme (France) based on 10 yr of
909 monitoring of their physicochemical properties, Atmos. Chem. Phys., 14, 1485-1506,
910 doi: 10.5194/acp-14-1485-2014, 2014.

911 Demoz, B. B., Collett, J. L., and Daube, B. C.: On the Caltech Active Strand Cloudwater
912 Collectors, Atmos. Res., 41, 47-62, doi: 10.1016/0169-8095(95)00044-5, 1996.

913 Draxler, R. R., and Rolph, G. D.: HYSPLIT (HYbrid Single-Particle Lagrangian Integrated
914 Trajectory) Model access via NOAA ARL READY Website
915 (http://www.arl.noaa.gov/ready/hysplit4.html). NOAA Air Resources Laboratory,
916 Silver Spring, MD, 2003.

917 EEA: European Union emission inventory report 1990–2012 under the UNECE Convention
918 on Long-range Transboundary Air Pollution (LRTAP), European Environment
919 Agency (EEA), Luxembourg, Technical Report 12/2014, 130 pp., doi: 10.2800/18374,
920 2014.

921 Elbert, W., Hoffmann, M. R., Kramer, M., Schmitt, G., and Andreae, M. O.: Control of solute
922 concentrations in cloud and fog water by liquid water content, Atmos. Environ., 34,
923 1109-1122, doi: 10.1016/S1352-2310(99)00351-9, 2000.

924 Elbert, W., Kramer, M., and Andreae, M. O.: Reply to discussion on "Control of solute
925 concentrations in cloud and fog water by liquid water content", Atmos. Environ., 36,
926 1909-1910, doi: Pii S1352-2310(02)00143-7

927 10.1016/S1352-2310(02)00143-7, 2002.

928 Facchini, M. C., Mircea, M., Fuzzi, S., and Charlson, R. J.: Cloud albedo enhancement by
929 surface-active organic solutes in growing droplets, Nature, 401, 257-259, doi:
930 10.1038/45758, 1999.

931 Fahey, K. M., Pandis, S. N., Collett, J. L., and Herckes, P.: The influence of size-dependent
932 droplet composition on pollutant processing by fogs, Atmos. Environ., 39, 4561-4574,
933 doi: 10.1016/j.atmosenv.2005.04.006, 2005.

934 Flossmann, A. I., and Wobrock, W.: A review of our understanding of the aerosol–cloud
935 interaction from the perspective of a bin resolved cloud scale modelling, Atmos. Res.,
936 97, 478-497, doi: 10.1016/j.atmosres.2010.05.008, 2010.

Fowler, D., Pilegaard, K., Sutton, M. A., Ambus, P., Raivonen, M., Duyzer, J., Simpson, D., Fagerli, H., Fuzzi, S., Schjoerring, J. K., Granier, C., Neftel, A., Isaksen, I. S. A., Laj, P., Maione, M., Monks, P. S., Burkhardt, J., Daemmgen, U., Neirynck, J., Personne, E., Wichink-Kruit, R., Butterbach-Bahl, K., Flechard, C., Tuovinen, J. P., Coyle, M., Gerosa, G., Loubet, B., Altimir, N., Gruenhage, L., Ammann, C., Cieslik, S., Paoletti, E., Mikkelsen, T. N., Ro-Poulsen, H., Cellier, P., Cape, J. N., Horvath, L., Loreto, F., Niinemets, U., Palmer, P. I., Rinne, J., Misztal, P., Nemitz, E., Nilsson, D., Pryor, S., Gallagher, M. W., Vesala, T., Skiba, U., Brueggemann, N., Zechmeister-Boltenstern, S., Williams, J., O'Dowd, C., Facchini, M. C., de Leeuw, G., Flossman, A., Chaumerliac, N., and Erisman, J. W.: Atmospheric composition change: Ecosystems-Atmosphere interactions, Atmos. Environ., 43, 5193-5267, doi: 10.1016/j.atmosenv.2009.07.068, 2009.

Gilardoni, S., Massoli, P., Giulianelli, L., Rinaldi, M., Paglione, M., Pollini, F., Lanconelli, C., Poluzzi, V., Carbone, S., Hillamo, R., Russell, L. M., Facchini, M. C., and Fuzzi, S.: Fog scavenging of organic and inorganic aerosol in the Po Valley, Atmos. Chem. Phys., 14, 6967-6981, doi: 10.5194/acp-14-6967-2014, 2014.

Giulianelli, L., Gilardoni, S., Tarozzi, L., Rinaldi, M., Decesari, S., Carbone, C., Facchini, M. C., and Fuzzi, S.: Fog occurrence and chemical composition in the Po valley over the last twenty years, Atmos. Environ., 98, 394-401, doi: 10.1016/j.atmosenv.2014.08.080, 2014.

Gurciullo, C. S., and Pandis, S. N.: Effect of composition variations in cloud droplet populations on aqueous-phase chemistry, J. Geophys. Res. - Atmos., 102, 9375-9385, doi: 10.1029/96jd03651, 1997.

Harris, E., Sinha, B., van Pinxteren, D., Tilgner, A., Fomba, K. W., Schneider, J., Roth, A., Gnauk, T., Fahlbusch, B., Mertes, S., Lee, T., Collett, J., Foley, S., Borrmann, S., Hoppe, P., and Herrmann, H.: Enhanced Role of Transition Metal Ion Catalysis During In-Cloud Oxidation of SO2, Science, 340, 727-730, doi: 10.1126/science.1230911, 2013.

Harris, E., Sinha, B., van Pinxteren, D., Schneider, J., Poulain, L., Collett, J., D'Anna, B., Fahlbusch, B., Foley, S., Fomba, K. W., George, C., Gnauk, T., Henning, S., Lee, T., Mertes, S., Roth, A., Stratmann, F., Borrmann, S., Hoppe, P., and Herrmann, H.: In-cloud sulfate addition to single particles resolved with sulfur isotope analysis during HCCT-2010, Atmos. Chem. Phys., 14, 4219-4235, doi: 10.5194/acp-14-4219-2014, 2014.

Hayden, K. L., Macdonald, A. M., Gong, W., Toom-Sauntry, D., Anlauf, K. G., Leithead, A., Li, S. M., Leaitch, W. R., and Noone, K.: Cloud processing of nitrate, J. Geophys. Res. - Atmos., 113, -, doi: 10.1029/2007jd009732, 2008.

Hegg, D. A., Hobbs, P. V., and Radke, L. F.: Measurements of the Scavenging of Sulfate and Nitrate in Clouds, Atmos. Environ., 18, 1939-1946, doi: 10.1016/0004-6981(84)90371-8, 1984.

Hegg, D. A., Gao, S., and Jonsson, H.: Measurements of selected dicarboxylic acids in marine cloud water, Atmos. Res., 62, 1-10, doi: 10.1016/S0169-8095(02)00023-6, 2002.

Herckes, P., Wendling, R., Sauret, N., Mirabel, P., and Wortham, H.: Cloudwater studies at a high elevation site in the Vosges Mountains (France), Environ. Pollut., 117, 169-177, doi: 10.1016/S0269-7491(01)00139-7, 2002.

Herckes, P., Valsaraj, K. T., and Collett, J. L.: A review of observations of organic matter in fogs and clouds: Origin, processing and fate, Atmos. Res., 132-133, 434-449, doi: 10.1016/j.atmosres.2013.06.005, 2013.

Herrmann, H., Wolke, R., Müller, K., Brüggemann, E., Gnauk, T., Barzaghi, P., Mertes, S., Lehmann, K., Massling, A., Birmili, W., Wiedensohler, A., Wieprecht, W., Acker, K., Jaeschke, W., Kramberger, H., Svrcina, B., Bächmann, K., Collett, J. L., Galgon, D., Schwirn, K., Nowak, A., van Pinxteren, D., Plewka, A., Chemnitzer, R., Rüd, C., Hofmann, D., Tilgner, A., Diehl, K., Heinold, B., Hinneburg, D., Knoth, O., Sehili, A. M., Simmel, M., Wurzler, S., Majdik, Z., Mauersberger, G., and Müller, F.: FEBUKO and MODMEP: Field measurements and modelling of aerosol and cloud multiphase processes, Atmospheric Environment, 39, 4169-4183, 2005.

Herrmann, H., Schaefer, T., Tilgner, A., Styler, S. A., Weller, C., Teich, M., and Otto, T.: Tropospheric Aqueous-Phase Chemistry: Kinetics, Mechanisms, and Its Coupling to a Changing Gas Phase, Chem. Rev., 150507133427007, doi: 10.1021/cr500447k, 2015.

Hitzenberger, R., Berner, A., Kromp, R., Kasper-Giebl, A., Limbeck, A., Tscherwenka, W., and Puxbaum, H.: Black carbon and other species at a high-elevation European site (Mount Sonnblick, 3106 m, Austria): Concentrations and scavenging efficiencies, J. Geophys. Res. - Atmos., 105, 24637-24645, doi: 10.1029/2000jd900349, 2000.

Hoag, K. J., Collett, J. L., and Pandis, S. N.: The influence of drop size-dependent fog chemistry on aerosol processing by San Joaquin Valley fogs, Atmos. Environ., 33, 4817-4832, doi: 10.1016/S1352-2310(99)00268-X, 1999.

Joos, F., and Baltensperger, U.: A Field-Study on Chemistry, S(IV) Oxidation Rates and Vertical Transport during Fog Conditions, Atmospheric Environment Part a-General Topics, 25, 217-230, doi: 10.1016/0960-1686(91)90292-F, 1991.

Kasper-Giebl, A., Koch, A., Hitzenberger, R., and Puxbaum, H.: Scavenging efficiency of 'aerosol carbon' and sulfate in supercooled clouds at Mt. Sonnblick (3106 m a.s.l., Austria), J. Atmos. Chem., 35, 33-46, doi: 10.1023/A:1006250508562, 2000.

Kasper-Giebl, A.: Control of solute concentrations in cloud and fog water by liquid water content, Atmos. Environ., 36, 1907-1908, doi: 10.1016/S1352-2310(02)00147-4, 2002.

Khwaja, H. A.: Atmospheric concentrations of carboxylic acids and related compounds at a semiurban site, Atmos. Environ., 29, 127-139, doi: 10.1016/1352-2310(94)00211-3, 1995.

Laj, P., Fuzzi, S., Facchini, M. C., Lind, J. A., Orsi, G., Preiss, M., Maser, R., Jaeschke, W., Seyffer, E., Helas, G., Acker, K., Wieprecht, W., Moller, D., Arends, B. G., Mols, J. J., Colvile, R. N., Gallagher, M. W., Beswick, K. M., Hargreaves, K. J., StoretonWest, R. L., and Sutton, M. A.: Cloud processing of soluble gases, Atmos. Environ., 31, 2589-2598, doi: 10.1016/S1352-2310(97)00040-X, 1997.

Lammel, G., and Metzig, G.: Multiphase Chemistry of Orographic Clouds - Observations at Sub-Alpine Mountain Sites, Fresen. J. Anal. Chem., 340, 564-574, doi: 10.1007/Bf00322431, 1991.

Lazrus, A. L., Kok, G. L., Gitlin, S. N., Lind, J. A., and McLaren, S. E.: Automated fluorimetric method for hydrogen peroxide in atmospheric precipitation, Anal. Chem., 57, 917-922, doi: 10.1021/ac00281a031, 1985.

1026 Leaitch, W. R., Strapp, J. W., Wiebe, H. A., Anlauf, K. G., and Isaac, G. A.: Chemical and
1027 Microphysical Studies of Nonprecipitating Summer Cloud in Ontario, Canada, J.
1028 Geophys. Res. - Atmos., 91, 1821-1831, doi: 10.1029/Jd091id11p11821, 1986.

1029 Löflund, M., Kasper-Giebl, A., Schuster, B., Giebl, H., Hitzenberger, R., and Puxbaum, H.:
1030 Formic, acetic, oxalic, malonic and succinic acid concentrations and their contribution
1031 to organic carbon in cloud water, Atmos. Environ., 36, 1553-1558, 2002.

1032 Marinoni, A., Laj, P., Sellegri, K., and Mailhot, G.: Cloud chemistry at the Puy de Dome:
1033 variability and relationships with environmental factors, Atmos. Chem. Phys., 4, 715-
1034 728, 2004.

1035 Marinoni, A., Parazols, M., Brigante, M., Deguillaume, L., Amato, P., Delort, A.-M., Laj, P.,
1036 and Mailhot, G.: Hydrogen peroxide in natural cloud water: Sources and
1037 photoreactivity, Atmos. Res., 101, 256-263, doi: 10.1016/j.atmosres.2011.02.013,
1038 2011.

1039 Mertes, S., Galgon, D., Schwirn, K., Nowak, A., Lehmann, K., Massling, A., Wiedensohler,
1040 A., and Wieprecht, W.: Evolution of particle concentration and size distribution
1041 observed upwind, inside and downwind hill cap clouds at connected flow conditions
1042 during FEBUKO, Atmos. Environ., 39, 4233-4245, doi:
1043 10.1016/j.atmosenv.2005.02.009, 2005.

1044 Möller, D., Acker, K., and Wieprecht, W.: A relationship between liquid water content and
1045 chemical composition in clouds, Atmos. Res., 41, 321-335, doi: 10.1016/0169-
1046 8095(96)00017-8, 1996.

1047 Moore, K. F., Sherman, D. E., Reilly, J. E., and Collett, J. L.: Development of a multi-stage
1048 cloud water collector Part 1: Design and field performance evaluation, Atmos.
1049 Environ., 36, 31-44, doi: 10.1016/S1352-2310(01)00476-9, 2002.

1050 Moore, K. F., Sherman, D. E., Reilly, J. E., and Collett, J. L.: Drop size-dependent chemical
1051 composition in clouds and fogs. Part I. Observations, Atmos. Environ., 38, 1389-1402,
1052 doi: 10.1016/j.atmosenv.2003.12.013, 2004a.

1053 Moore, K. F., Sherman, D. E., Reilly, J. E., Hannigan, M. P., Lee, T., and Collett, J. L.: Drop
1054 size-dependent chemical composition of clouds and fogs. Part II: Relevance to
1055 interpreting the aerosol/trace gas/fog system, Atmos. Environ., 38, 1403-1415, doi:
1056 10.1016/j.atmosenv.2003.12.014, 2004b.

1057 Neuman, J. A., Huey, L. G., Ryerson, T. B., and Fahey, D. W.: Study of Inlet Materials for
1058 Sampling Atmospheric Nitric Acid, Environ. Sci. Technol., 33, 1133-1136, doi:
1059 10.1021/es980767f, 1999.

1060 Noone, K. J., Ogren, J. A., Hallberg, A., Heintzenberg, J., Strom, J., Hansson, H.-C.,
1061 Svenningsson, B., Wiedensohler, A., Fuzzi, S., Facchini, M. C., Arends, B. G., and
1062 Berner, A.: Changes in aerosol size- and phase distributions due to physical and
1063 chemical processes in fog, Tellus B, 44, 489-504, doi: 10.1034/j.1600-0889.1992.t01-
1064 4-00004.x, 1992.

1065 Ogren, J. A., and Charlson, R. J.: Implications for models and measurements of chemical
1066 inhomogeneities among cloud droplets, Tellus B, 44, 208-225, doi: 10.1034/j.1600-
1067 0889.1992.t01-2-00004.x, 1992.

1068 Ogren, J. A., Noone, K. J., Hallberg, A., Heintzenberg, J., Schell, D., Berner, A., Solly, I.,
1069 Kruisz, C., Reischl, G., Arends, B. G., and Wobrock, W.: Measurements of the size

dependence of the concentration of nonvolatile material in fog droplets, Tellus B, 44, 570-580, doi: 10.1034/j.1600-0889.1992.t01-1-00010.x, 1992.

Phillips, G. J., Makkonen, U., Schuster, G., Sobanski, N., Hakola, H., and Crowley, J. N.: The detection of nocturnal N2O5 as HNO3 by alkali- and aqueous-denuder techniques, Atmos. Meas. Techn., 6, 231-237, doi: 10.5194/amt-6-231-2013, 2013.

Prabhakar, G., Ervens, B., Wang, Z., Maudlin, L. C., Coggon, M. M., Jonsson, H. H., Seinfeld, J. H., and Sorooshian, A.: Sources of nitrate in stratocumulus cloud water: Airborne measurements during the 2011 E-PEACE and 2013 NiCE studies, Atmos. Environ., 97, 166-173, doi: 10.1016/j.atmosenv.2014.08.019, 2014.

Pruppacher, H. R., and Klett, J. D.: Concentrations of water soluble compounds in individual cloud and raindrops, chapter 17.3 in: Microphysics of clouds and precipitation, 2nd ed., Springer, New York, 954 pp., 2010.

R Core Team: R: A language and environment for statistical computing: http://www.R-project.org, 2015.

Raja, S., Raghunathan, R., Yu, X. Y., Lee, T. Y., Chen, J., Kommalapati, R. R., Murugesan, K., Shen, X., Qingzhong, Y., Valsaraj, K. T., and Collett, J. L.: Fog chemistry in the Texas-Louisiana Gulf Coast corridor, Atmos. Environ., 42, 2048-2061, doi: 10.1016/j.atmosenv.2007.12.004, 2008.

Raja, S., Raghunathan, R., Kommalapati, R. R., Shen, X. H., Collett, J. L., and Valsaraj, K. T.: Organic composition of fogwater in the Texas-Louisiana gulf coast corridor, Atmos. Environ., 43, 4214-4222, doi: 10.1016/j.atmosenv.2009.05.029, 2009.

Rao, X., and Collett, J. L.: Behavior of S(Iv) and Formaldehyde in a Chemically Heterogeneous Cloud, Environ. Sci. Technol., 29, 1023-1031, doi: 10.1021/es00004a024, 1995.

Reilly, J. E., Rattigan, O. V., Moore, K. F., Judd, C., Sherman, D. E., Dutkiewicz, V. A., Kreidenweis, S. M., Husain, L., and Collett, J. L.: Drop size-dependent S(IV) oxidation in chemically heterogeneous radiation fogs, Atmos. Environ., 35, 5717-5728, doi: 10.1016/S1352-2310(01)00373-9, 2001.

Roth, A., Schneider, J., Klimach, T., Mertes, S., van Pinxteren, D., Herrmann, H., and Borrmann, S.: Aerosol properties, source identification, and cloud processing in orographic clouds measured by single particle mass spectrometry on a Central European mountain site during HCCT-2010, Atmospheric Chemistry and Physics, accepted 19 December 2015, doi: 10.5194/acp-16-1-2016, 2016.

Rumsey, I. C., Cowen, K. A., Walker, J. T., Kelly, T. J., Hanft, E. A., Mishoe, K., Rogers, C., Proost, R., Beachley, G. M., Lear, G., Frelink, T., and Otjes, R. P.: An assessment of the performance of the Monitor for AeRosols and GAses in ambient air (MARGA): a semi-continuous method for soluble compounds, Atmos. Chem. Phys., 14, 5639-5658, doi: 10.5194/acp-14-5639-2014, 2014.

Schell, D., Wobrock, W., Maser, R., Preiss, M., Jaeschke, W., Georgii, H. W., Gallagher, M. W., Bower, K. N., Beswick, K. M., Pahl, S., Facchini, M. C., Fuzzi, S., Wiedensohler, A., Hansson, H. C., and Wendisch, M.: The size-dependent chemical composition of cloud droplets, Atmos. Environ., 31, 2561-2576, doi: 10.1016/S1352-2310(96)00286-5, 1997.

1113 Schwarzenböck, A., Heintzenberg, J., and Mertes, S.: Incorporation of aerosol particles
1114 between 25 and 850 nm into cloud elements: measurements with a new
1115 complementary sampling system, Atmos. Res., 52, 241-260, 2000.

1116 Seinfeld, J. H., and Pandis, S. N.: Atmospheric chemistry and physics : From air pollution to
1117 climate change -2nd edition, 2nd ed., Wiley, New York, 1326 pp., 2006.

1118 Sellegri, K.: Size-dependent scavenging efficiencies of multicomponent atmospheric aerosols
1119 in clouds, J. Geophy. Res., 108, doi: 10.1029/2002jd002749, 2003.

1120 Sellegri, K., Laj, P., Marinoni, A., Dupuy, R., Legrand, M., and Preunkert, S.: Contribution of
1121 gaseous and particulate species to droplet solute composition at the Puy de Dome,
1122 France, Atmos. Chem. Phys., 3, 1509-1522, 2003.

1123 Spiess, A.-N., and Neumeyer, N.: An evaluation of R2 as an inadequate measure for nonlinear
1124 models in pharmacological and biochemical research: a Monte Carlo approach, BMC
1125 Pharmacology, 10, doi: 10.1186/1471-2210-10-6, 2010.

1126 Straub, D. J., and Collett, J. L.: Development of a multi-stage cloud water collector Part 2:
1127 Numerical and experimental calibration, Atmos. Environ., 36, 45-56, doi:
1128 10.1016/S1352-2310(01)00477-0, 2002.

1129 Straub, D. J., Hutchings, J. W., and Herckes, P.: Measurements of fog composition at a rural
1130 site, Atmos. Environ., 47, 195-205, doi: 10.1016/j.atmosenv.2011.11.014, 2012.

1131 Svenningsson, B., Hansson, H. C., Martinsson, B., Wiedensohler, A., Swietlicki, E.,
1132 Cederfelt, S. I., Wendisch, M., Bower, K. N., Choularton, T. W., and Colvile, R. N.:
1133 Cloud droplet nucleation scavenging in relation to the size and hygroscopic behaviour
1134 of aerosol particles, Atmos. Environ., 31, 2463-2475, doi: 10.1016/S1352-
1135 2310(96)00179-3, 1997.

1136 Taraniuk, I., Kostinski, A. B., and Rudich, Y.: Enrichment of surface-active compounds in
1137 coalescing cloud drops, Geophys. Res. Lett., 35, -, doi: 10.1029/2008gl034973, 2008.

1138 Tilgner, A., Schöne, L., Bräuer, P., van Pinxteren, D., Hoffmann, E., Spindler, G., Styler, S.
1139 A., Mertes, S., Birmili, W., Otto, R., Merkel, M., Weinhold, K., Wiedensohler, A.,
1140 Deneke, H., Schrödner, R., Wolke, R., Schneider, J., Haunold, W., Engel, A., Wéber,
1141 A., and Herrmann, H.: Comprehensive assessment of meteorological conditions and
1142 airflow connectivity during HCCT-2010, Atmos. Chem. Phys., 14, 9105-9128, doi:
1143 10.5194/acp-14-9105-2014, 2014.

1144 van Pinxteren, D., Plewka, A., Hofmann, D., Müller, K., Kramberger, H., Svrcina, B.,
1145 Bächmann, K., Jaeschke, W., Mertes, S., Collett, J. L., and Herrmann, H.: Schmücke
1146 hill cap cloud and valley stations aerosol characterisation during FEBUKO (II):
1147 Organic compounds, Atmos. Environ., 39, 4305-4320, doi:
1148 10.1016/j.atmosenv.2005.02.014, 2005.

1149 van Pinxteren, D., Brüggemann, E., Gnauk, T., Iinuma, Y., Müller, K., Nowak, A., Achtert,
1150 P., Wiedensohler, A., and Herrmann, H.: Size- and time-resolved chemical particle
1151 characterization during CAREBeijing-2006: Different pollution regimes and diurnal
1152 profiles, J. Geophys. Res. - Atmos., 114, doi: 10.1029/2008jd010890, 2009.

1153 van Pinxteren, D., Brüggemann, E., Gnauk, T., Müller, K., Thiel, C., and Herrmann, H.: A
1154 GIS based approach to back trajectory analysis for the source apportionment of
1155 aerosol constituents and its first application, J. Atmos. Chem., 67, 1-28, doi:
1156 10.1007/s10874-011-9199-9, 2010.

Vet, R., Artz, R. S., Carou, S., Shaw, M., Ro, C.-U., Aas, W., Baker, A., Bowersox, V. C., Dentener, F., Galy-Lacaux, C., Hou, A., Pienaar, J. J., Gillett, R., Forti, M. C., Gromov, S., Hara, H., Khodzher, T., Mahowald, N. M., Nickovic, S., Rao, P. S. P., and Reid, N. W.: A global assessment of precipitation chemistry and deposition of sulfur, nitrogen, sea salt, base cations, organic acids, acidity and pH, and phosphorus, Atmos. Environ., 93, 3-100, doi: 10.1016/j.atmosenv.2013.10.060, 2014.

Whalley, L. K., Stone, D., George, I. J., Mertes, S., van Pinxteren, D., Tilgner, A., Herrmann, H., Evans, M. J., and Heard, D. E.: The influence of clouds on radical concentrations: observations and modelling studies of HOx during the Hill Cap Cloud Thuringia (HCCT) campaign in 2010, Atmos. Chem. Phys., 15, 3289-3301, doi: 10.5194/acp-15-3289-2015, 2015.

Wickham, H.: ggplot2: Elegant graphics for data analysis, Springer, New York, 2009.

Wrzesinsky, T., and Klemm, O.: Summertime fog chemistry at a mountainous site in central Europe, Atmos. Environ., 34, 1487-1496, doi: 10.1016/S1352-2310(99)00348-9, 2000.

Zimmermann, L., and Zimmermann, F.: Fog deposition to Norway Spruce stands at high-elevation sites in the Eastern Erzgebirge (Germany), J. Hydrol., 256, 166-175, doi: 10.1016/S0022-1694(01)00532-7, 2002.

Tables and Figures

Table 1: Sampling times of cloud water collectors during Full Cloud Events with mean liquid water content (LWC), droplet surface area (PSA), effective droplet radius (R_{eff}), Schmücke above cloud base (SACB), temperature (T), wind speed (WS), and global radiation (GR) at Mt. Schmücke, as well as the number of samples for the different collectors.

Event	Start (CEST)	Stop (CEST)	Duration (h)	LWC ($g\ m^{-3}$)	SACB (m)	PSA ($cm^2\ m^{-3}$)	R_{eff} (µm)	T (°C)	WS ($m\ s^{-1}$)	GR ($W\ m^{-2}$)	# CASCC2	# 3-stage	# 5-stage
FCE1.1	14/09/2010 11:00	15/09/2010 02:00	15	0.24	167	1248	5.7	9.2	8.2	15	15	7	-[a]
FCE7.1	24/09/2010 23:45	25/09/2010 01:45	2	0.19	156	846	5.7	8.3	5.5	0	2	1	1
FCE11.2	01/10/2010 22:30	02/10/2010 05:30	7	0.37	237	1277	8.7	6.2	4.1	0	7	4	4
FCE11.3	02/10/2010 14:30	02/10/2010 19:30	5	0.33	225	1353	7.4	7.7	7.3	31	5	3	2
FCE13.3	06/10/2010 12:15	07/10/2010 03:15	15	0.34	185	1392	7.3	9.1	3.9	52	15	8	4
FCE22.1	19/10/2010 21:30	20/10/2010 03:30	6	0.30	222	1272	7.4	1.2	4.7	0	6	3	2
FCE26.1	24/10/2010 01:30	24/10/2010 08:30	7	0.20	174	961	7.6	2.3	8.9	0	7	3	-[a]
FCE26.2	24/10/2010 09:15	24/10/2010 11:45	2.5	0.14	141	701	7.3	1.4	9.1	43	3	1	-[a]

a) Collector not operated

Table 2: Summary of cloud water solute concentrations determined during HCCT-2010.

Compound	Unit	#	Range	median	mean	VWM
pH		60	3.6-5.3	4.56	4.29[a]	4.30[a]
SO_4^{2-}	µmol L^{-1}	60	6.2-104	33	43	39
NO_3^-	µmol L^{-1}	60	46-479	151	164	142
Cl^-	µmol L^{-1}	60	3.7-84	22	30	25
NH_4^+	µmol L^{-1}	60	64-523	182	216	191
Na^+	µmol L^{-1}	60	0.58-195	20	35	27
K^+	µmol L^{-1}	60	1.3-31	3.8	6.1	5.5
Mg^{2+}	µmol L^{-1}	60	0.63-26	3.1	5.1	4.1
Ca^{2+}	µmol L^{-1}	60	1.4-37	7	9.8	8.7
H_2O_2	µmol L^{-1}	60	0.35-17	5	5.6	5.4
S(IV)	µmol L^{-1}	34	BDL-3.6	2.1	1.9	1.9
HMS	µmol L^{-1}	34	BDL-2.7	0.76	0.87	0.91
DOC	mgC L^{-1}	60	1.3-13	4	4.4	3.9

#: Number of samples analysed
VWM: volume-weighted mean concentration
BDL: below detection limit
[a] derived from mean/VWM H^+ concentration

Table 3: Comparison of mean HCCT-2010 cloud water concentrations with literature data (arithmetic or volume-weighted means) from other European mountain sites.

Location	Date	pH	Cl^- (μM)	SO_4^{2-} (μM)	NO_3^- (μM)	NH_4^+ (μM)	Na^+ (μM)	K^+ (μM)	Mg^{2+} (μM)	Ca^{2+} (μM)	H_2O_2 (μM)	DOC (mg L^{-1})	S(IV) (μM)	Ref.
Schmücke, Germany	2010	4.3	30	43	164	216	35	6.1	5.1	9.8	5.6	4.4	1.9	This work
Puy de Dome, France[a]	2001-2011	4.3	69	60	417	233	44	18	3.8	53	4.9	12[d]		(Deguillaume et al., 2014)
Puy de Dome, France[b]	2001-2011	5.1	35	49	111	145	34	5.0	6.6	15	10	5.5[d]		(Deguillaume et al., 2014)
Sudety Mts., Poland	2003-2004	4.25	66	67	173	167	67	6	10	26				(Blas et al., 2008)
Schmücke, Germany	2001-2002	4.5	19	59	207						2.7	6.4		(Brüggemann et al., 2005)
Holme Moss, UK[c]	1994-2001		652-1711	90-208[e]	175-469	158-518	578-1563							(Beswick et al., 2003)
Rax, Austria	1999-2000	3.8	16	82	136	230	16	7	11	11		6.0[d]		(Löflund et al., 2002)
Vosges Mts., France	1998-1999	4.82	143	149	181	276	175	57	26	60				(Herckes et al., 2002)
Zinnwald, Germany	1997-1998	4.0	48	281	176	560	52	23	6	28				(Zimmermann and Zimmermann, 2002)
Waldstein, Germany	1997	4.3	54	248	481	669	65	11.5	19.5	34				(Wrzesinsky and Klemm, 2000)
Krusne Hory, Czech Rep.	1995-1996	2.96	155	625	726	203	64	20	20	68				(Bridges et al., 2002)
Brocken, Germany[c]	1992-1996	3.8-4.5	68-119	133-160	280-365	378-468	60-128	2-12	14-18	27-67				(Acker et al., 1998)
Great Dun Fell, UK	1993	4.0		91	202	321							2.7	(Laj et al., 1997)
Sonnblick, Austria	1991[f]	4.5	30	64	32	36	34	12	2.9	11				(Brantner et al., 1994)
Vosges Mts., France	1990	3.3	120	185	410	270	170	40					24	(Lammel and Metzig, 1991)
Schöllkopf, Germany	1988	4.1	90	250	400	830	70	60						(Lammel and Metzig, 1991)
Zindelen, Switzerland	1986-1987	4.8	431	447	1020	2107							85.9	(Joos and Baltensperger, 1991)

a) polluted regime
b) continental regime
c) range of annual means
d) TOC
e) nss-Sulfate
f) fall data

Table 4: Factor loadings of 4 principal components after Varimax rotation. Loadings with absolute values < 0.2 are regarded insignificant and omitted, while those > 0.6 are regarded highly significant and printed bold.

	F1	F2	F3	F4
pH		0.53	-0.26	-0.36
LWC	-0.57	-0.32		0.47
Reff	-0.45	**-0.74**		
RTI Water	**0.84**		-0.48	
RTI NaturalVegetation	**-0.92**		0.28	
RTI Agriculture	-0.39		**0.63**	0.49
RTI Urban	0.22			**0.91**
Sulfate		**0.93**		
Nitrate		**0.73**	0.54	0.24
Ammonium		**0.97**		
Sodium	**0.95**			
Magnesium	**0.89**		0.24	0.20
Chloride	**0.95**			
Potassium			**0.87**	
Calcium	0.26	0.34	**0.72**	0.34
DOC	-0.24	**0.77**	0.50	

Table 5: Event means of upwind and in-cloud scavenging efficiencies calculated from different approaches. Numbers in brackets include both particulate and gaseous upwind concentrations, where available. See text for details.

Event	CASCC2+MARGA	CASCC2+INT-AMS	CVI/INT AMS
Ammonium			
FCE1.1	0.85 (0.39)	0.92	0.83
FCE11.2	0.95 (0.52)	0.98	0.96
FCE11.3	1.04 (0.5)	0.97	0.97
FCE13.3	0.94 (0.65)	0.80	0.71
FCE22.1	0.85 (0.69)	0.96	0.96
FCE26.1+2	1.01 (0.51)	0.95	0.90
Nitrate			
FCE1.1	0.87 (0.82)	0.95	0.86
FCE11.2	2.26 (1.86)	0.99	0.95
FCE11.3	1.16 (1.01)	0.96	0.96
FCE13.3	1.17 (1.1)	0.87	0.79
FCE22.1	1.25 (1.18)	0.98	0.96
FCE26.1+2	1.04 (0.94)	0.96	0.94
Sulfate			
FCE1.1	0.66	0.88	0.79
FCE11.2	0.55	0.79	0.69
FCE11.3	0.79	0.89	0.88
FCE13.3	0.89	0.68	0.56
FCE22.1	0.82	0.94	0.94
FCE26.1+2	0.75	0.94	0.91
DOC			
FCE1.1	1.09a	0.83	0.67
FCE11.2	3.42a	0.86	0.88
FCE11.3	1.86a	0.89	0.92
FCE13.3	1.11a	0.72	0.69
FCE22.1	1.72a	0.87	0.79
FCE26.1+2	1.45a	0.89	0.86

a) DOC from MARGA not available. PM_{10} water-soluble organic carbon from Berner impactor used instead.

Figures

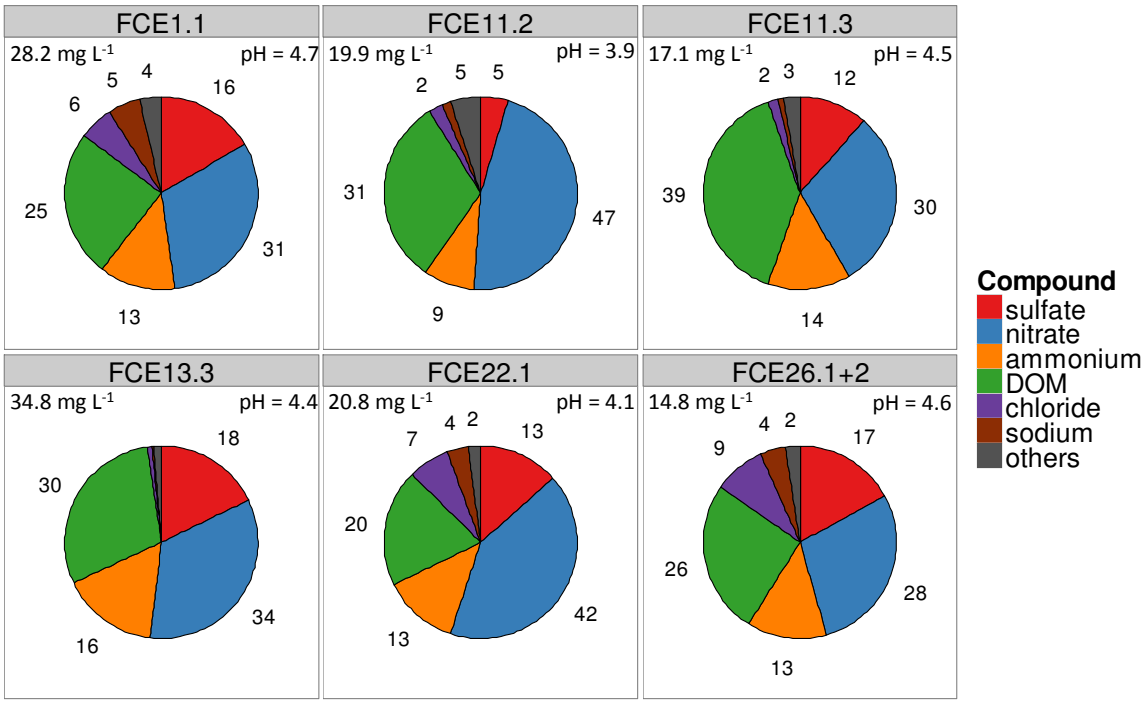

Figure 1: Volume-weighted mean composition of bulk cloud water during main events. Numbers represent percentage from total solute concentration (in mg L^{-1}). Trace solutes calcium, magnesium, potassium, H_2O_2(aq), and S(IV) are summarised as „others". DOM is calculated as DOC*1.8. Total solute concentrations and pH values derived from VWM H^+ concentrations are indicated in the upper left and reight panel corners, respectively.

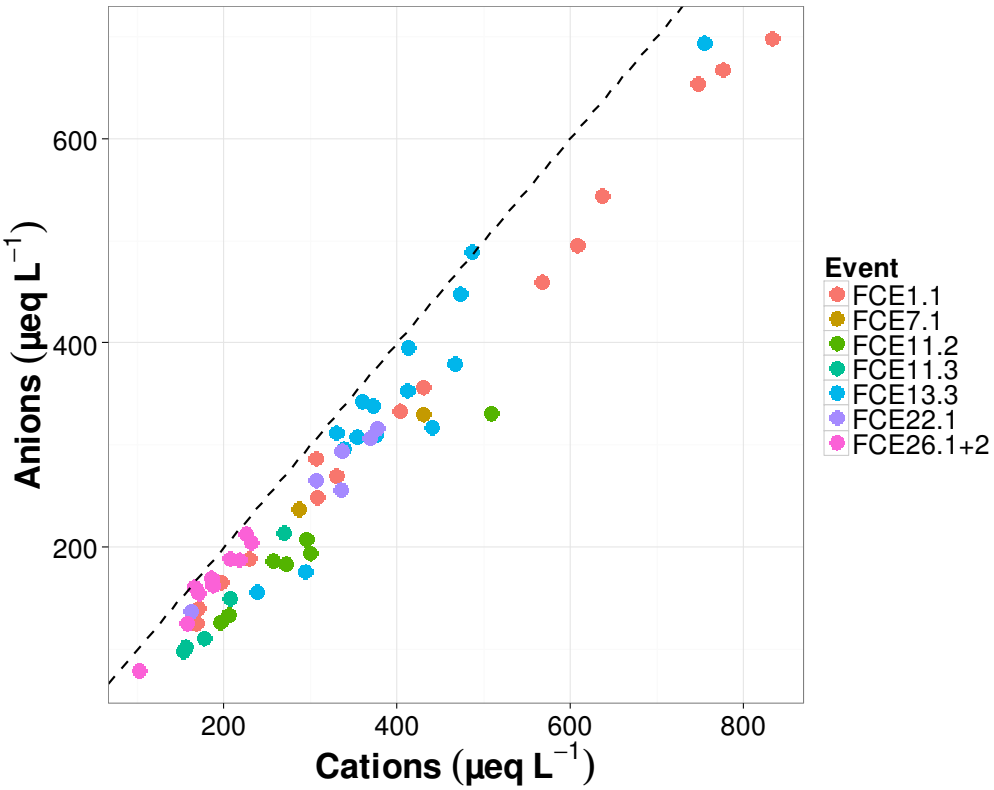

Figure 2: Ion balance on an equivalent basis for inorganic anions and cations. Dashed line is 1:1.

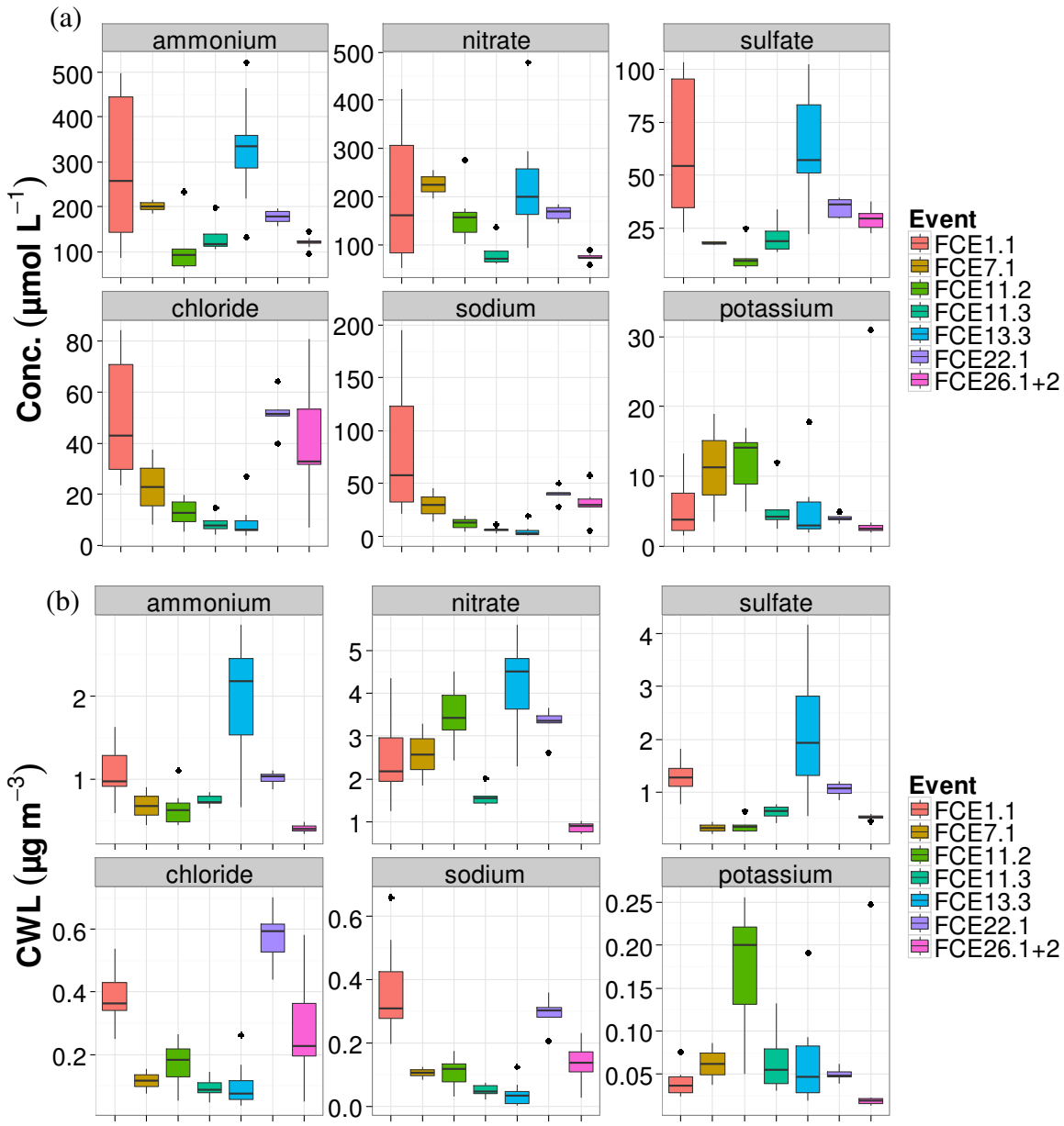

Figure 3: Variability of cloud water concentrations both within and between FCEs for selected inorganic ions. (a) Solute concentrations, (b) Cloud water loadings. Boxes indicate 25th, 50th, and 75th percentile, whiskers extend to 1.5 * IQR (interquartile range), and dots indicate individual data points outside this range.

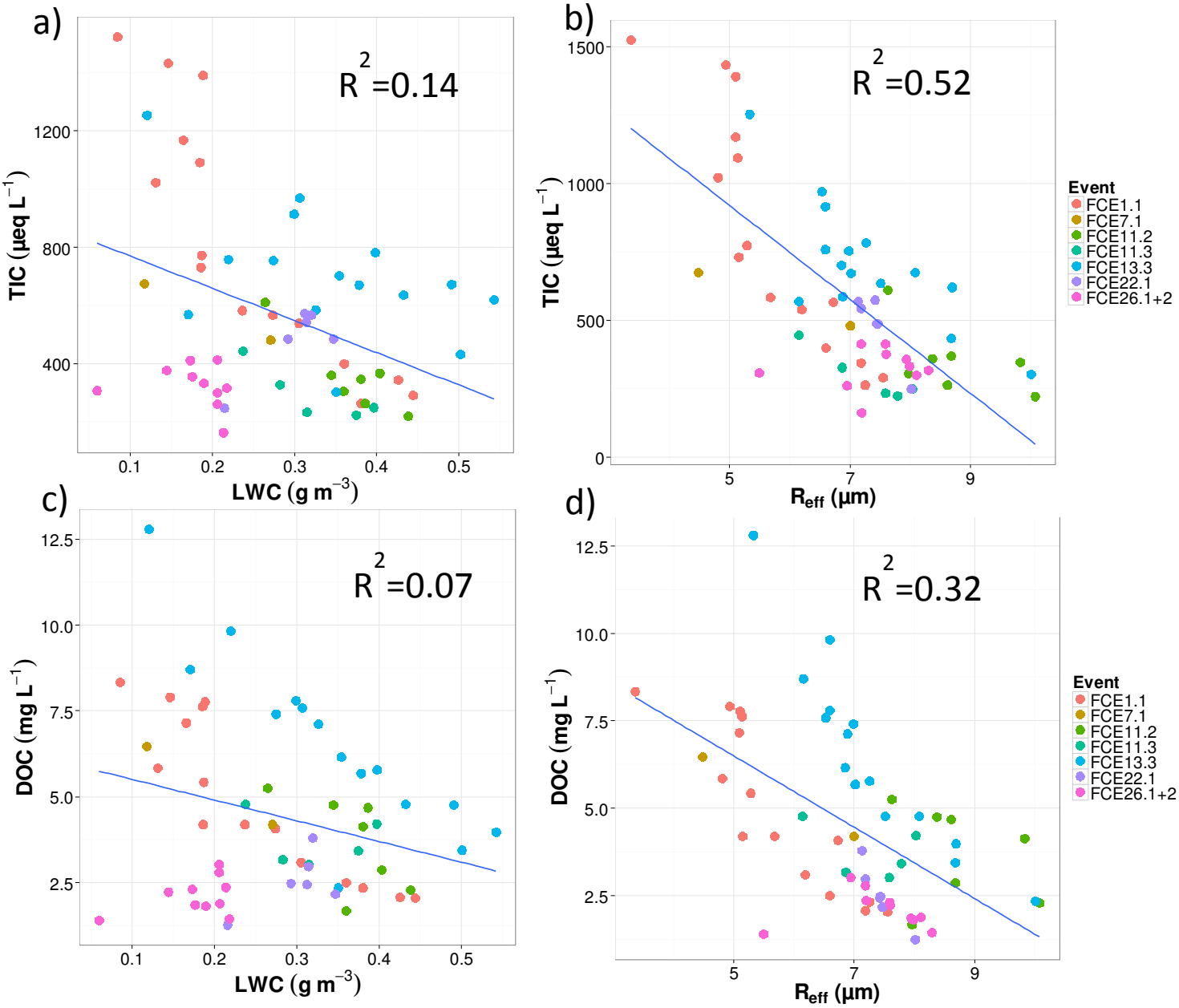

Figure 4: Relationships of total ionic content (upper panels) and dissolved organic carbon (lower panels) versus liquid water content (a and c) and effective droplet radius (b and d) for bulk cloud water samples.

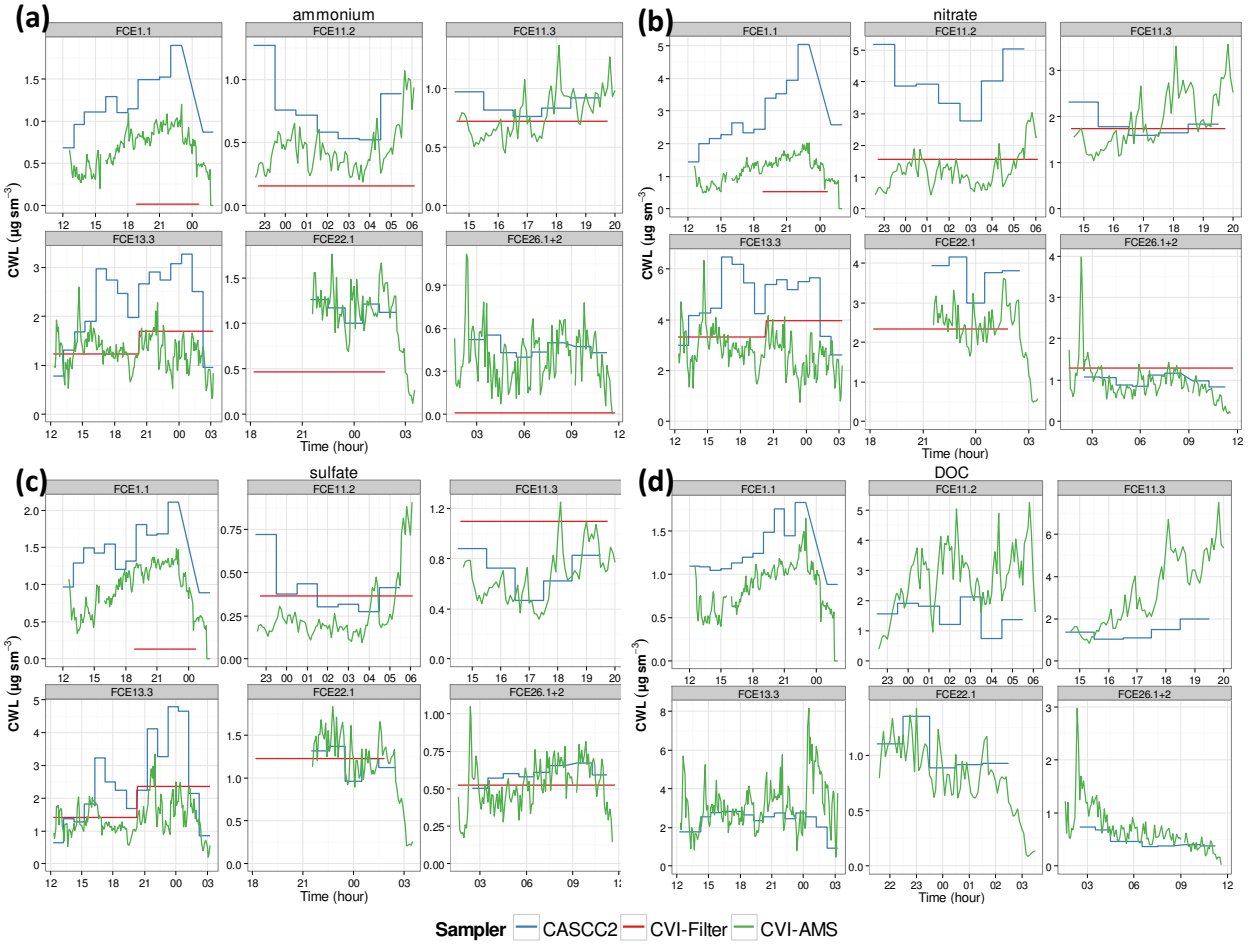

Figure 5: Comparison of cloud water loadings (normalised to standard temperature and pressure) from bulk cloud water collector (blue), quartz filter downstream CVI inlet (red), and AMS downstream CVI (green) for cloud water main constituents (a) ammonium, (b) nitrate, (c) sulfate, and (d) DOC (AMS organics/1.8).

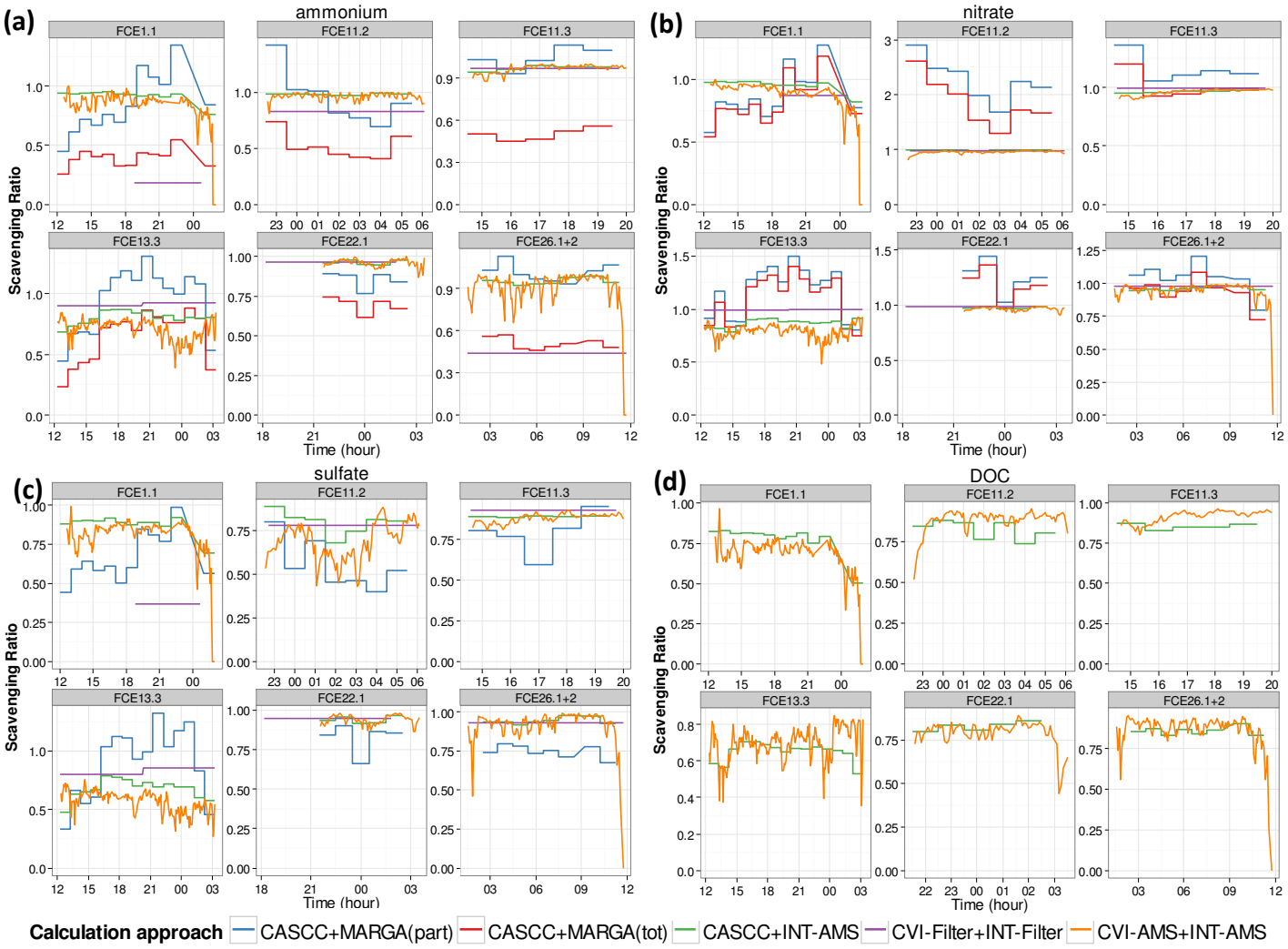

Figure 6: Cloud scavenging efficiencies for (a) ammonium, (b) nitrate, (c) sulfate, and (d) DOC, calculated as "upwind SE" from bulk cloud water loadings and upwind MARGA data (blue and red for MARGA particulate and total aerosol conentrations, respectively) and "in-cloud SEs" from bulk CWLs and interstitial AMS data (green), droplet residual and interstitial particle concentrations from filters (purple), and droplet residual and interstitial particle concentrations from AMS (orange). See text for details.

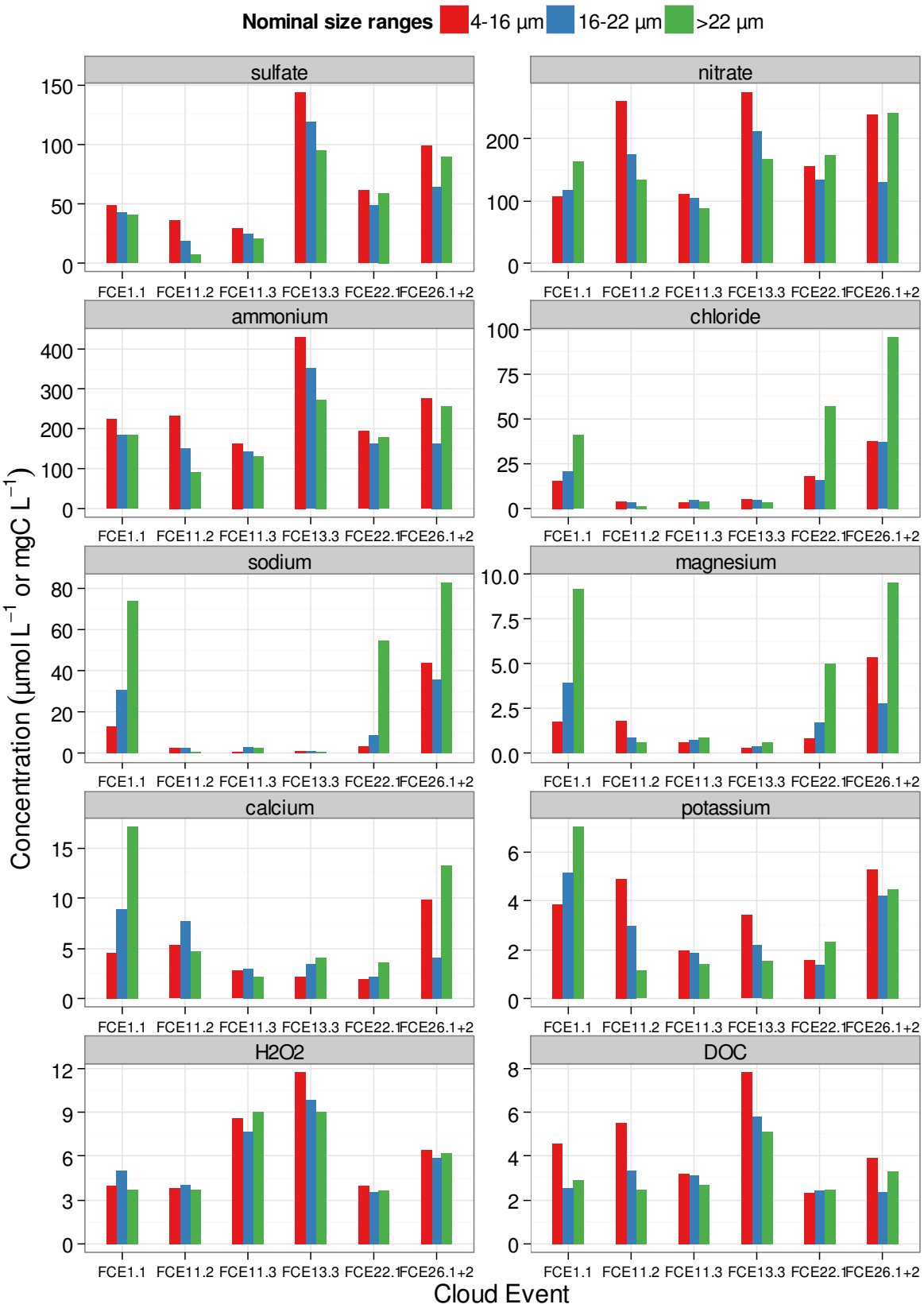

Figure 7: Size-resolved cloud water concentrations from 3-stage collector. Volume-weighted mean concentrations per event are given in µmol L^{-1} except for DOC (mgC L^{-1}).

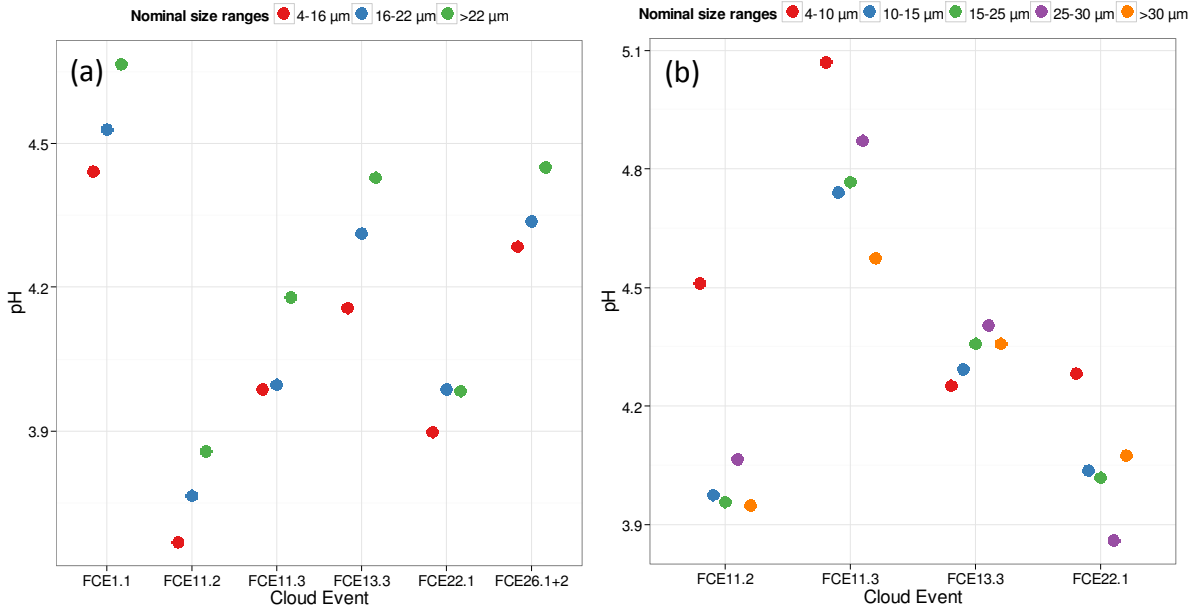

Figure 8: Mean pH values per event, calculated from volume-weighted mean concentrations of H^+ from (a) 3-stage cloud water collector, and (b) 5-stage collector.

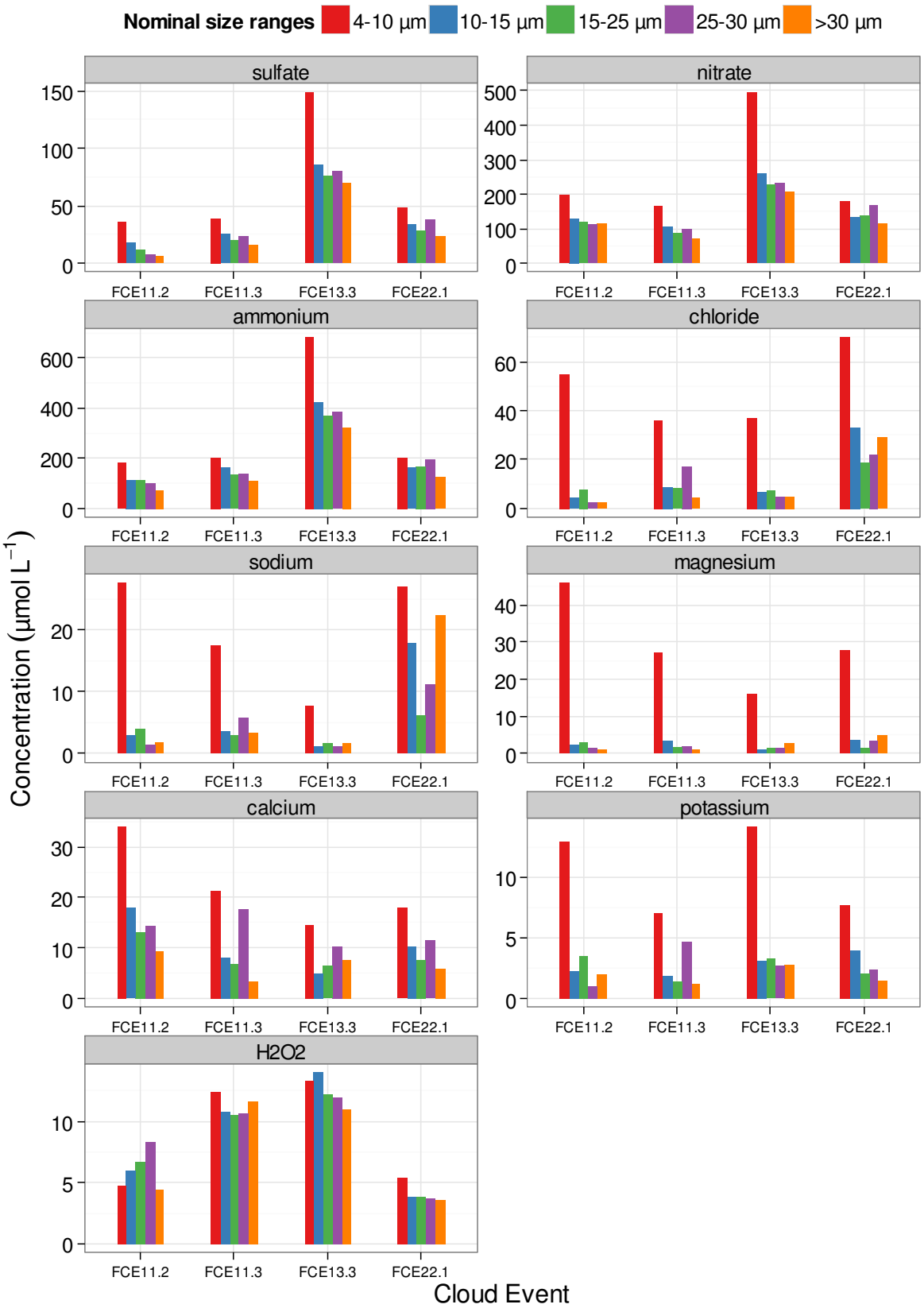

Figure 9: Size-resolved cloud water concentrations from 5-stage collector. Volume-weighted mean concentrations per event are given in µmol L^{-1}.